Available online at www.sciencedirect.com
ScienceDirect
Marine Micropaleontology 67 (2008) 46–68
MARINE MICROPALEONTOLOGY
www.elsevier.com/locate/marmicro

Benthic foraminiferal response to changes in bottom-water oxygenation and organic carbon flux in the eastern Mediterranean during LGM to Recent times

Ramadan H. Abu-Zied [a,b,*], Eelco J. Rohling [b], Frans J. Jorissen [c,d], Christophe Fontanier [c,d], James S.L. Casford [e], Steve Cooke [b,f]

[a] Geology Department, Faculty of Science, Mansoura University, El-Mansoura: 35516, Egypt
[b] School of Ocean and Earth Science, National Oceanography Centre, Southampton SO14 3ZH, UK
[c] Laboratory of Recent and Fossil Bio-Indicators (BIAF), UPRES EA 2644, Angers University, France
[d] LEBIM, Port Joinville, Ile d'Yeu, France
[e] Department of Geography, University of Durham, Science Site, Durham DH1 3LE, UK
[f] Department of Earth Sciences, the University of Waikato, Private Bag 3105, Hamilton 2001, New Zealand

Received 23 April 2007; received in revised form 18 August 2007; accepted 23 August 2007

Abstract

We present a high-resolution study of benthic foraminiferal abundances in 4 cores from the central Aegean and NE Levantine Seas, spanning the interval from 30 ka BP to the present. The benthic foraminiferal faunas indicate that during LGM times, bottom waters were well ventilated, while organic flux to the sea floor was significantly higher than today. From 30 to 10.2 ka BP, faunal density and composition suggest a gradual decrease in organic flux to the sea floor. This trend is interrupted by a short return to higher organic flux levels during the Younger Dryas (12.8–11.5 ka BP). The faunas immediately preceding the early to middle Holocene organic-rich layer (sapropel) S1 are very similar to Late Holocene faunas, indicating oligotrophic conditions. The transition from well ventilated bottom waters to anoxic (Levantine Basin) or strongly dysoxic (Aegean Sea) bottom waters appears to take place within a time-span of only 600 years, from ~10.8 to 10.2 ka BP. Sapropel S1 (10.2–6.4 ka BP) is characterized by extended periods of bottom-water anoxia in the Levantine Basin, and by strongly dysoxic conditions punctuated by episodic re-ventilation events in the Aegean Sea. Re-establishment of fully oxygenated bottom-water conditions after sapropel S1 was extremely rapid. The ensuing Late Holocene faunas are very similar to recent faunas found in the Aegean Sea, suggesting much lower fluxes of organic matter to the sea floor than during glacial times.

Keywords: benthic foraminifera; organic matter; sapropel; oligotrophic; Mediterranean

1. Introduction

The general absence of benthic foraminifera from most eastern Mediterranean sapropels (Parker, 1958; Cita, 1973; Kidd et al., 1978) suggests that anoxic conditions prevailed in the bottom waters at times of sapropel deposition (Van Straaten, 1972; Katz and

* Corresponding author. Geology Department, Faculty of Science, Mansoura University, El-Mansoura: 35516, Egypt. Tel.: +20 02 050 2242388; fax: +20 02 050 2247900.
E-mail address: rhaz@mans.edu.eg (R.H. Abu-Zied).

0377-8398/$ - see front matter © 2007 Elsevier B.V. All rights reserved.
doi:10.1016/j.marmicro.2007.08.006

Thunell, 1984; Nolet and Corliss, 1990; Rohling et al., 1997; Nijenhuis et al., 1996; Jorissen, 1999a). Bottom-water anoxia that precluded benthic life (Cita, 1973; Kidd et al., 1978; Cita and Podenzani, 1980; Mullineaux and Lohmann, 1981; Nolet and Corliss, 1990; Lander Rasmussen, 1991; Vismara-Schilling and Coulbourn, 1991) are commonly explained as a function of dissolved oxygen utilization during re-mineralization of organic matter (Berger and Wefer, 1990), exacerbated by reduced deep-water formation rates (Mangini and Schlosser, 1986; Rossignol-Strick, 1985; Rohling and Gieskes, 1989; Rohling, 1994). Enhanced organic matter flux and/or preservation leads to increased sedimentary organic carbon concentrations, a key characteristic of sapropels (cf. Kidd et al., 1978; Sigl et al., 1978; Anastasakis and Stanley, 1984).

In cores from shallower water (typically <2000 m), some benthic foraminiferal species, such as *Globobulimina affinis* and *Chilostomella mediterranensis*, persist throughout sapropels, suggesting that there were no persistent anoxia but that conditions instead remained severely dysoxic to intermittently anoxic (Van der Zwaan, 1980; Mullineaux and Lohmann, 1981; Katz and Thunell, 1984; Nolet and Corliss, 1990; Rohling et al., 1993, 1997; Jorissen, 1999a; Mercone et al., 2001; Casford et al., 2003). Jorissen (1999a) discussed benthic foraminiferal successions across several Late Quaternary Mediterranean sapropels and concluded that occurrences of faunas dominated by *Globobulimina* and *Chilostomella* around truly azoic levels are indicative of gradual decreases or increases in bottom-water oxygenation, while the presence of faunas dominated by small biconvex trochospiral taxa in post-sapropel sediments would reflect a rapid re-oxygenation of the benthic environment after sapropel formation.

At present, it is widely accepted that open-ocean benthic foraminiferal distribution patterns are mainly controlled by the organic carbon flux reaching the seafloor from surface-water productivity, and by the amount of dissolved oxygen in bottom/pore waters (e.g. Miller and Lohmann, 1982; Corliss, 1985 and 1991; Gooday, 1986; Corliss and Chen, 1988; Altenbach and Sarnthein, 1989; Van der Zwaan and Jorissen, 1991; Herguera and Berger, 1991; Barmawidjaja et al., 1992; Sen Gupta and Machain-Castillo, 1993; Jorissen et al., 1995 and 1998; Bernhard, 1996; Jannink et al., 1998; Jorissen, 1999b; Fontanier et al., 2002). Moreover, the quality and intensity of organic matter inputs are known to influence the species composition of foraminiferal assemblages, both along ocean margins and in central oceanic regions (Lutze and Coulbourn, 1984; Caralp, 1989; Loubere, 1991; Goldstein and Corliss, 1994). In areas of oligotrophy, there is commonly food limitation but no oxygen limitation, and the benthic foraminiferal ecosystem is relatively enriched in epifaunal species, whereas under more eutrophic conditions there is no food limitation but an increasing potential for oxygen limitation, and infaunal species tend to dominate (Jorissen et al., 1995; Jorissen, 1999b). In the modern oligotrophic eastern Mediterranean, there is no oxygen limitation, so that food availability should form the dominant control on benthic foraminiferal abundances. This expectation is borne out by observations. Decreasing primary productivity values from west to east through the Mediterranean

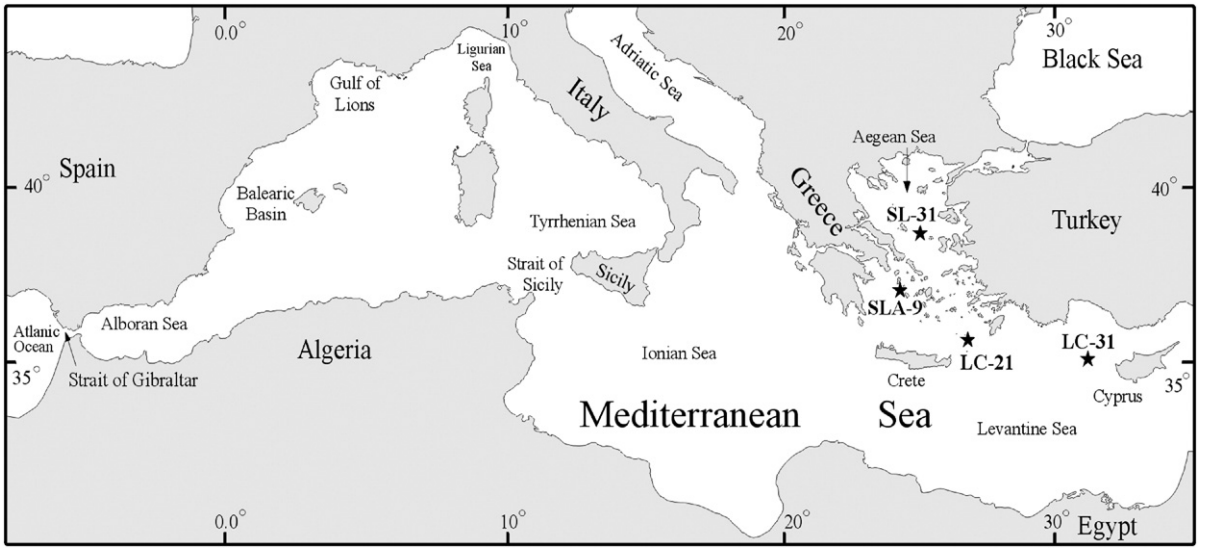

Fig. 1. Location map of the studied cores (LC-31, LC-21, SL-31 and SLA-9) in the Mediterranean Sea. Star symbol indicates the core site.

(Antoine et al., 1995) result in a similar west to east decrease in organic flux to the seafloor and, therefore, in a west to east decrease of food availability to the benthic foraminiferal community at comparable water depths. This west to east decrease in food availability is clearly reflected in the faunal compositions (De Rijk et al., 1999b, 2000), with more eutrophic species having a wider bathymetrical range in the west, and more oligotrophic species occurring at much shallower water depth in the eastern Mediterranean (De Rijk et al., 2000).

Within the sediments, the vertical distribution of benthic foraminifera is also controlled by oxygen and food (organic matter) availability (Corliss and Emerson, 1990; Jorissen et al., 1995; Jorissen, 1999b). An epifaunal habitat is considered to be advantageous in a food-limited environment with high oxygen levels (Corliss and Chen, 1988; Corliss, 1991; Jorissen et al., 1995). Infaunal taxa are found where there is an abundance of food, despite the associated lower pore-water oxygen concentrations (Corliss and Chen, 1988). It has been found that infaunal species abundance maxima may shift towards the sediment–water interface, tracking required pore-water oxygen levels (Jorissen, 1999b). For example, Barmawidjaja et al. (1992), have found that, in the Adriatic Sea, *Bolivina dilatata*, *Bolivina spathulata*, *Bulimina marginata* and *Hopkinsina pacifica* occur near the sediment surface in some months (October and December) and at deep infaunal positions in months that are characterized by improved bottom and pore-water oxygenation (February). These taxa are characterized by biserial or triserial coiling, and 'on average' are considered to inhabit shallow-infaunal microhabitats (Corliss, 1991; De Stigter et al., 1998; Jorissen, 1999a).

Here we use new benthic foraminiferal species abundance records, and comparison with previously published $\delta^{18}O$ and $\delta^{13}C$ data for various planktonic and benthic species in the same cores (Casford et al., 2002, 2003), to determine the history of dissolved oxygen and organic matter availability in the Aegean and NE Levantine upper slope to deep-sea environments from the last glacial maximum (LGM) to the Present, including the time of deposition of early Holocene sapropel S1. The inferred history of eastern Mediterranean deep-water ventilation is compared with previous reconstructions of regional surface-water and climate conditions.

2. Materials and methods

We have studied four cores (SL-31, SLA-9, LC-2l and LC-31) from the central Aegean Sea to the NE Levantine Sea (W-NW of Cyprus) (Fig. 1). Cores SL-31

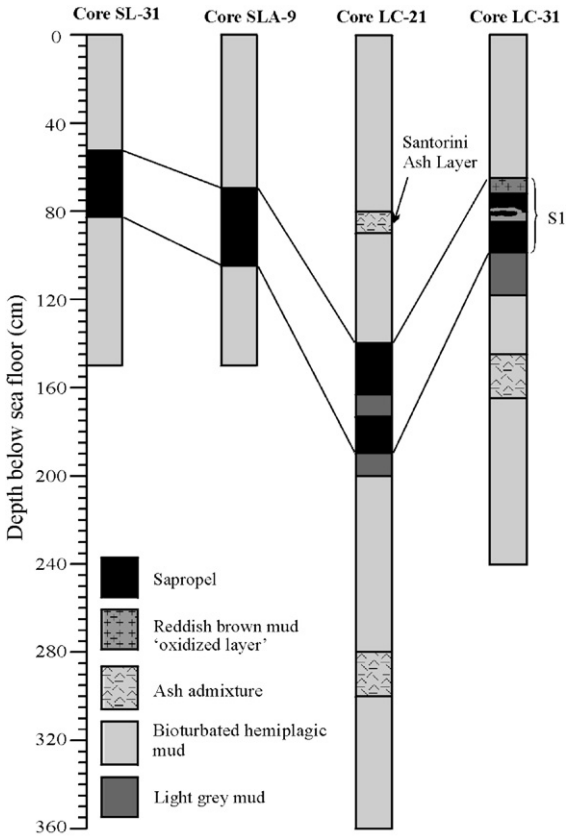

Fig. 2. Lithological characteristics of core SL-31, SLA-9, LC-21 and LC-31.

and SLA-9 are gravity cores from 38° 56′ N and 25° 00′ E in the north-central Aegean Basin and 37° 31′ N and 34° 33′ E in the southwestern Aegean Basin, at present-day water depths of 430 and 260 m, respectively. They were recovered by *R.V. Aegeo* in May 1998. SL-31 and SLA-9 were sampled in U-channels on board ship, and all material has since been depleted. Cores LC-21 and LC-31 are long piston cores that were recovered during *R.V. Marion Dufresne* Cruise *81* (17 January–9 February 1995). Core LC-21 is located at 35° 39.71′ N and 26° 34.96′ E, north–east of Crete at a present-day water depth of 1520 m. Core LC-31 is located at 34° 59.76′ N and 31° 09.81′ E, west-northwest of Cyprus at a present-day water depth of 2300 m. Cores LC-21 and LC-31 are archived at the BOSCORF core repository, National Oceanography Centre, Southampton.

3. Lithology

Cores SL-31 and SLA-9 consist of light gray to brown homogeneous mud, interrupted by a dark, olive brown-green colored sapropelic layer (Holocene sapropel S1)

Table 1
AMS ^{14}C datings and their calibration into calendar years using the online version of Calib 5.01 (Stuiver et al., 2005); radiocarbon ages calibrated using the marine mode of the programme Calib 5.01 (Hughen et al., 2004)

Uncorrected depth (cm)	Corrected depth (cm)	AMS lab. code	Conventional ^{14}C age (ka BP)	Calibrated age (ka BP)	1σ-calibrated age range (ka BP)
Core SL-31:					
51.75	–	KIA9467	6.515±0.045	7.032	6.961–7.103
65.75	–	KIA9468	7.95±0.06	8.412	8.35–8.474
84.25	–	KIA9469	9.33±0.057	10.177	10.124–10.231
91	–	KIA9470	9.99±0.055	10.997	10.885–11.109
126.75	–	KIA9471	14.65±0.08	17.020	16.789–17.252
Core SLA-9:					
60.5	–	KIA9472	5.950±0.045	6.351	6.301–6.401
71.5	–	KIA9473	6.445±0.055	6.929	6.85–7.009
83.25	–	KIA9474	7.9±0.045	8.363	8.322–8.404
99.5	–	KIA9475	8.4±0.05	9.013	8.944–9.082
120.5	–	KIA9476	11.91±0.07	13.343	13.279–13.408
Core LC-21:					
50	50	CAMS-41314	3.37±0.06	3.224	3.14–3.308
95.5	85.5	CAMS-41313	4.29±0.06	4.419	4.333–4.506
137.75	127.75	CAMS-41311	5.59±0.06	5.981	5.904–6.058
161.5	151.5	CAMS-41315	7.48±0.06	7.935	7.872–7.998
174.25	164.25	CAMS-41312	8.12±0.06	8.595	8.506–8.684
190.5	179.5	AA-30364	9.01±0.07	9.674	9.558–9.79
219	209	AA-30365	11.77±0.08	13.233	13.164–13.302
252.5	242.5	CAMS-41316	14.45±0.06	16.747	16.545–16.949
Core LC-31:					
28.5	–	CAMS-45864	3.45±0.05	3.324	3.263–3.385
60.5	–	CAMS-45863	6.12±0.05	6.552	6.486–6.618
84.25	–	AA-30367	10.90±0.10	12.484	12.296–12.673
87.5	–	CAMS-45861	8.74±0.05	9.425	9.374–9.477
96.5	–	CAMS-45862	8.50±0.05	9.123	9.046–9.2
131.5	–	CAMS-45860	12.04±0.05	13.482	13.404–13.561
247.5	–	CAMS-45859	32.96±0.05	35.96	

between 82 and 52 cm and between 105 and 70 cm, respectively (Fig. 2). The lower 10 and 20 cm of the sapropelic layers in these two cores, respectively, are darker than the rest of the sapropelic layers. The sapropels display sharp transitions into the underlying and overlying sediments. The top 20 cm of the cores was visibly oxidized, and foraminiferal shells were sometimes covered with reddish to brown coatings. No such coatings were observed below 20 cm.

Core LC-21 consists mainly of light gray, bioturbated, foraminifera-rich hemipelagic mud that becomes brown-green between 200 and 191 cm (Fig. 2). A dark olive-green sapropel is found between 191 and 140 cm, with sharp transitions into the underlying and overlying light gray sediments. There has been little to no post-depositional re-oxidation ("burn-down") at the top of S1 in this core (Mercone et al., 2001). The sapropel consists of two sub-units that are separated by a gray layer between 173 and 163 cm depth, the so-called "sapropel interruption" (Rohling et al., 1997, 2002; De Rijk et al., 1999a; Mercone et al., 2001). A silt-sized volcanic ash layer between 91 and 81 cm represents the Z-2 ash layer from the Minoan eruption of Santorini (Keller et al., 1978; McCoy, 1980). Between 280 and 250 cm, the light gray pre-sapropel contains an admixture of clear volcanic ash shards that may represent Santorini ash layer Y-2 (Pichler and Friedrich, 1976; Keller et al., 1978; McCoy, 1980; Narcisi and Vezzoli, 1999).

Core LC-31 consists mainly of yellowish brown hemipelagic mud (Fig. 2). Between 165 and 145 cm, an admixture of coarse, glassy volcanic ash shards may again represent Santorini ash layer Y-2 (Pichler and Friedrich, 1976; Keller et al., 1978; Narcisi and Vezzoli, 1999). At 118 cm, the brown colors change into light gray hues that gradationally darken into the dark olive-green colors of the sapropel (S1) at 98 cm. Sapropel S1 continues up to 72 cm, where it ends with a sharp transition into reddish to dark brown mud. The sapropel layer is interrupted between 85 and 80 cm by two light gray colored layers. One of these layers crosses only half the width of the core, and is interpreted as a small slump. From 72 cm upward, the hemipelagic mud gradually

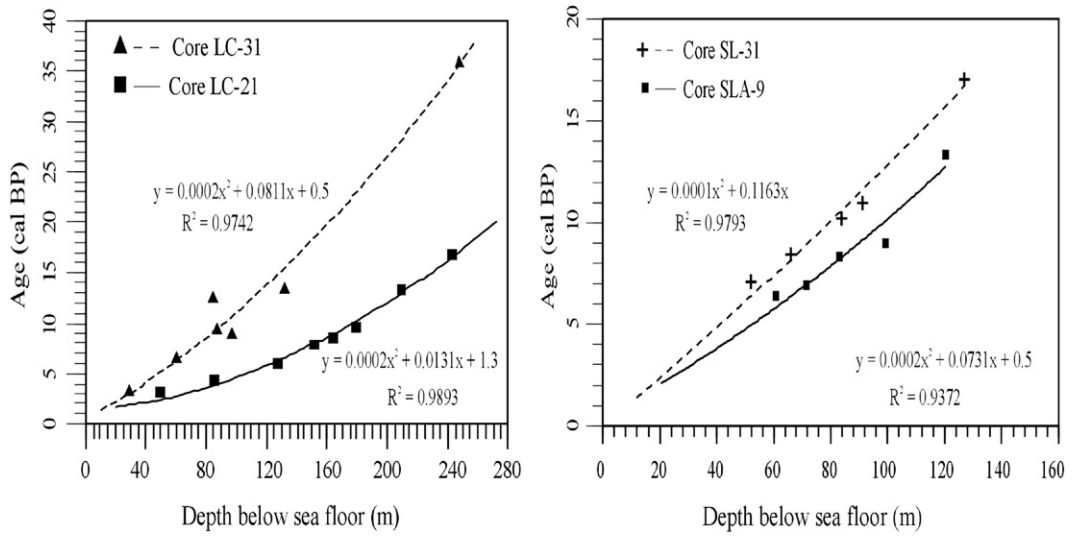

Fig. 3. Age-depth plots of cores LC-31, LC-21, SL-31, SLA-9. Ages are calibrated and plotted against original depths, except in core LC-21 where the age is plotted against depth corrected for 10 cm thickness of the Santorini ash layer found between 81 and 91 cm.

changes from reddish brown into yellowish brown colors around 65 cm.

4. Time-stratigraphic framework

Radiocarbon datings of the studied cores (Table 1) have been previously published by Mercone et al. (2000 and 2001), Casford et al. (2002) and Rohling et al. (2002). Here, we calibrated these AMS ^{14}C datings using the marine mode (Hughen et al., 2004) of the online version of Calib 5.01 (Stuiver et al., 2005). After calibration, all dating points (Table 1) are plotted against original depths, except in core LC-21, where the calibrated ages are plotted against depth (Fig. 3) corrected for 10 cm thickness of the Santorini ash layer (Fig. 2). The best regression lines for the calibrated dating points of each core have been obtained by using polynomial fitting (order 2) (Fig. 3). Subsequently, ages were determined for all samples by using the equations of these regression lines (Fig. 3).

5. Micropalaeontological analyses

Cores SL-31 and SLA-9 were sampled continuously in 0.5 cm intervals over their entire length. Core LC-21 was sampled every 5 cm for the top 50 cm interval, every 3 cm for the interval immediately above S1, in a continuous sequence of 1 cm intervals through S1, and every 7 cm in the pre-sapropel interval. Core LC-31 was sampled every 1 cm in the post-sapropel interval, continuously in 0.5 cm intervals through S1, at 1 cm spacing for the interval immediately below S1, and at 3 cm spacing for the rest of the core. All samples were dried for 24–48 h at 50 °C. Once dry, the samples were weighed, then soaked in distilled water and wet sieved in a sieve stack with mesh widths of 600 μm, 150 μm, 125 μm and 63 μm. Residues were dried again at 50 °C, and weighed in order to obtain the dry weight of each sieved fraction.

The entire 150–600 μm fraction has been used without any partitioning or splitting, in order to pick up to 250 specimens from each sample, or as many as present. Benthic foraminiferal specimens were identified and mounted in 64-cell slides. The key species have been listed in the Appendix A and displayed in Plates I II III. Species counts of cores LC-31 and LC-21 (Appendix B) have been presented as percentages of the total calcareous taxa, while the agglutinated taxa (e.g. *Glomospira charoides*, *Ammolagena clavata* and *Ammoglobigerina globigeriniformis*) are presented as percentages of the total fauna. The species counts of cores SL-31 and SLA-9 (Appendix B) are presented as a percentage of the total benthic foraminiferal fauna due to the absence of the above-mentioned agglutinates that have organic lining walls.

6. Faunal assemblage variations

Faunal abundance distributions are discussed per core, starting with the deep-sea cores, and finishing with the Aegean upper-slope cores. In this way, the cores are presented in trophic order, going from the most oligotrophic (deepest) ones to the most eutrophic (shallowest) ones.

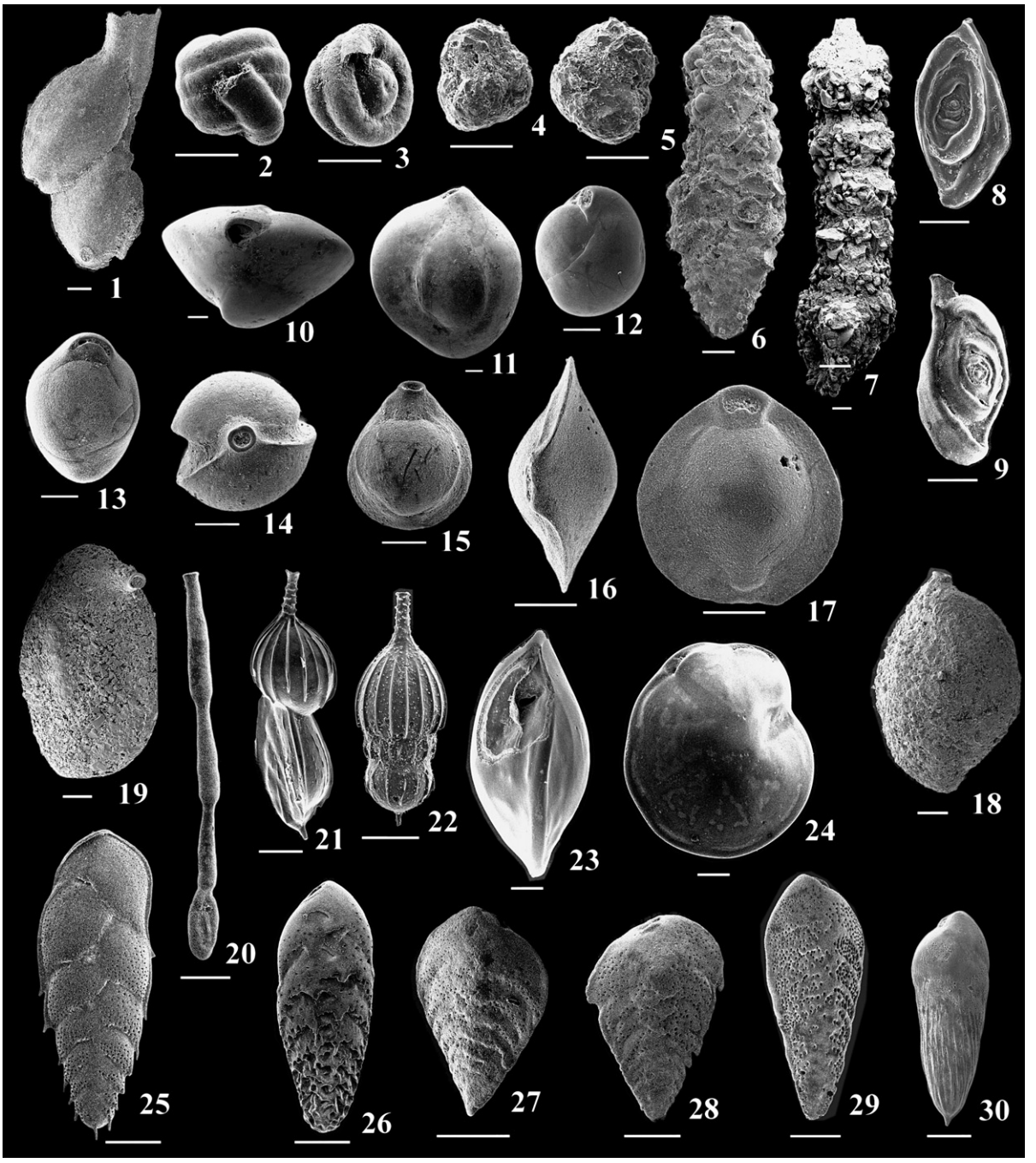

Plate I. 1, *Ammolagena clavata* (Jones & Parker). 2–3, *Glomospira charoides* (Jones & Parker). 4–5, *Ammoglobigerina globigeriniformis* (Parker & Jones). 6, *Bigenerina nodosaria* d'Orbigny, side view of adult specimen. 7, *Pseudoclavulina crustata* Cushman, side view. 8, *Spirophthalmidium acutimargo* (Brady), side view. 9, *Spirophthalmidium acutimargo concava* Heron-Allen & Earland, convex side view. 10–11, *Quinqueloculina lamarckiana* d'Orbigny: 10, apertural view; 11, side view. 12–13, *Miliolinella irregularis* (d'Orbigny), side views. 14–15, *Pyrgo lucernula* (Schwager): 14, apertural view; 15, side view. 16–17, *Pyrgo murrhina* (Schwager): 16, peripheral view; 17, side view. 18–19, *Sigmoilopsis schlumbergeri* (Silvestri), side views. 20, *Articulina tubulosa* (Seguenza), side view. 21–22, *Amphicoryna scalaris* (Batsch), side views. 23–24, *Hoeglundina elegans* (d'Orbigny): 23, peripheral view; 24, umbilical view. 25, *Bolivina alata* (Seguenza), side view. 26, *Bolivina albatrossi* Cushman, side view. 27–29, *B. spathulata* (Williamson), side views. 30, *Bolivina striatula* (Cushman), side view. Each scale bar represents 100 μm.

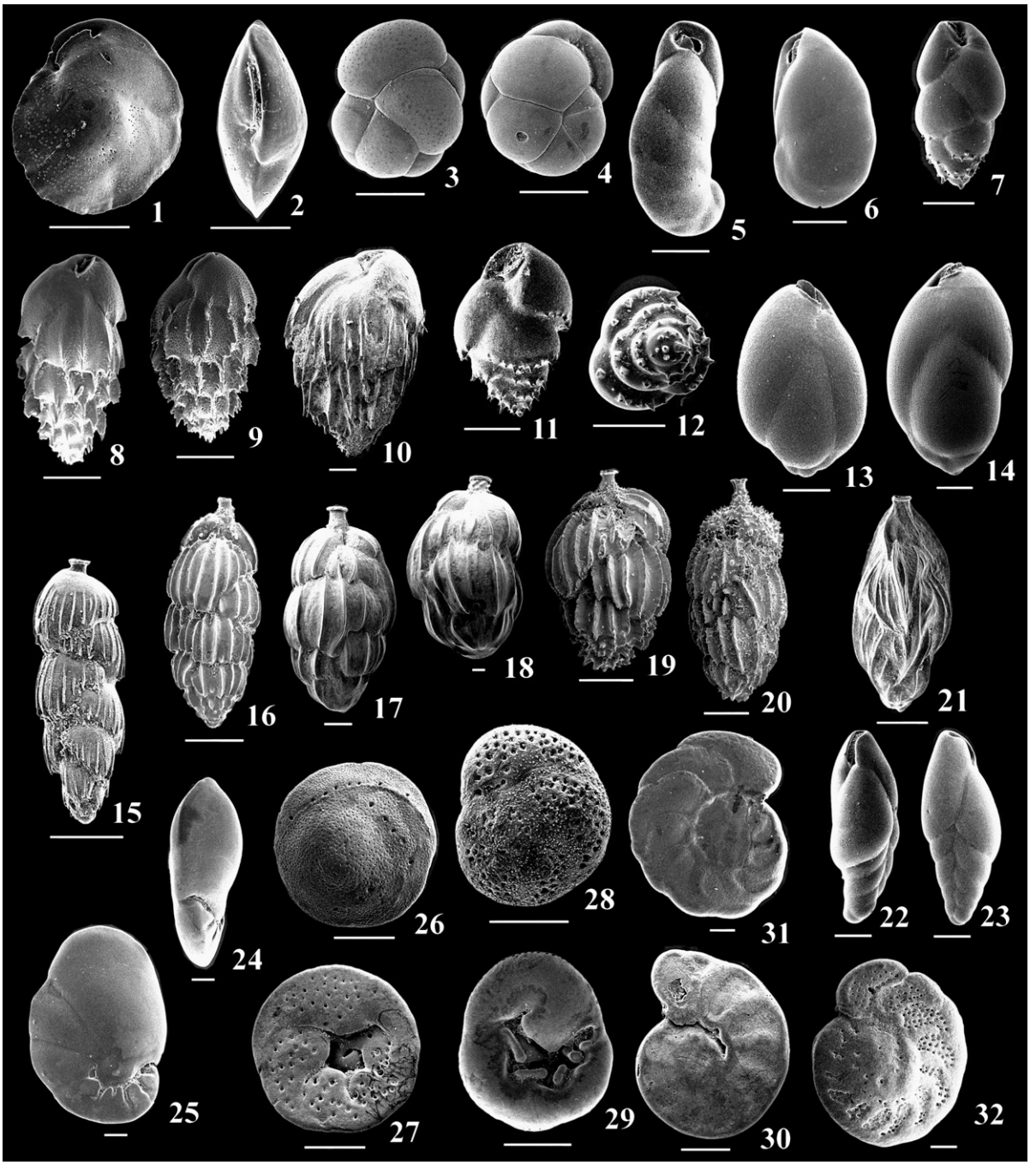

Plate II. 1–2, *Cassidulina carinata* Silvestri: 1, side view; 2, peripheral view. 3–4, *Cassidulina crassa* d'Orbigny, side views. 5–6, *Cassidulinoides bradyi* (Norman), side views. 7, *Bulimina aculeata* d'Orbigny, side view. 8–9, *Bulimina costata* d'Orbigny, side views. 10, *Bulimina inflata* Seguenza, side view. 11–12, *Bulimina marginata* d'Orbigny: 11, side view; 12, basal view showing the under cutting margins. 13–14, *Globobulimina affinis* (d'Orbigny), side views. 15, *Rectuvigerina phlegeri* Le Calvez, side view. 16, *Uvigerina bifurcata* d'Orbigny, side view. 17–18, *Uvigerina mediterranea* Hofker, side views. 19–20, *Uvigerina peregrina* Cushman, side views. 21, *Trifarina angulosa* (Williamson), side view. 22–23, *Rutherfordoides rotundiformis* (McCulloch): 22, peripheral view; 23, side view. 24–25, *Cancris auriculus* (Fichtel & Moll): 24, peripheral view; 25, umbilical view. 26–27, *Neoconorbina terquemi* (Rzehak): 26, spiral view; 27, umbilical view. 28–29, *Rosalina bradyi* (Cushman): 28, spiral view; 29, umbilical view. 30, *Hyalinea balthica* (Schroeter), umbilical view. 31–32, *Planulina ariminensis* d'Orbigny: 31, spiral view; 32, umbilical view. Each scale bar represents 100 μm.

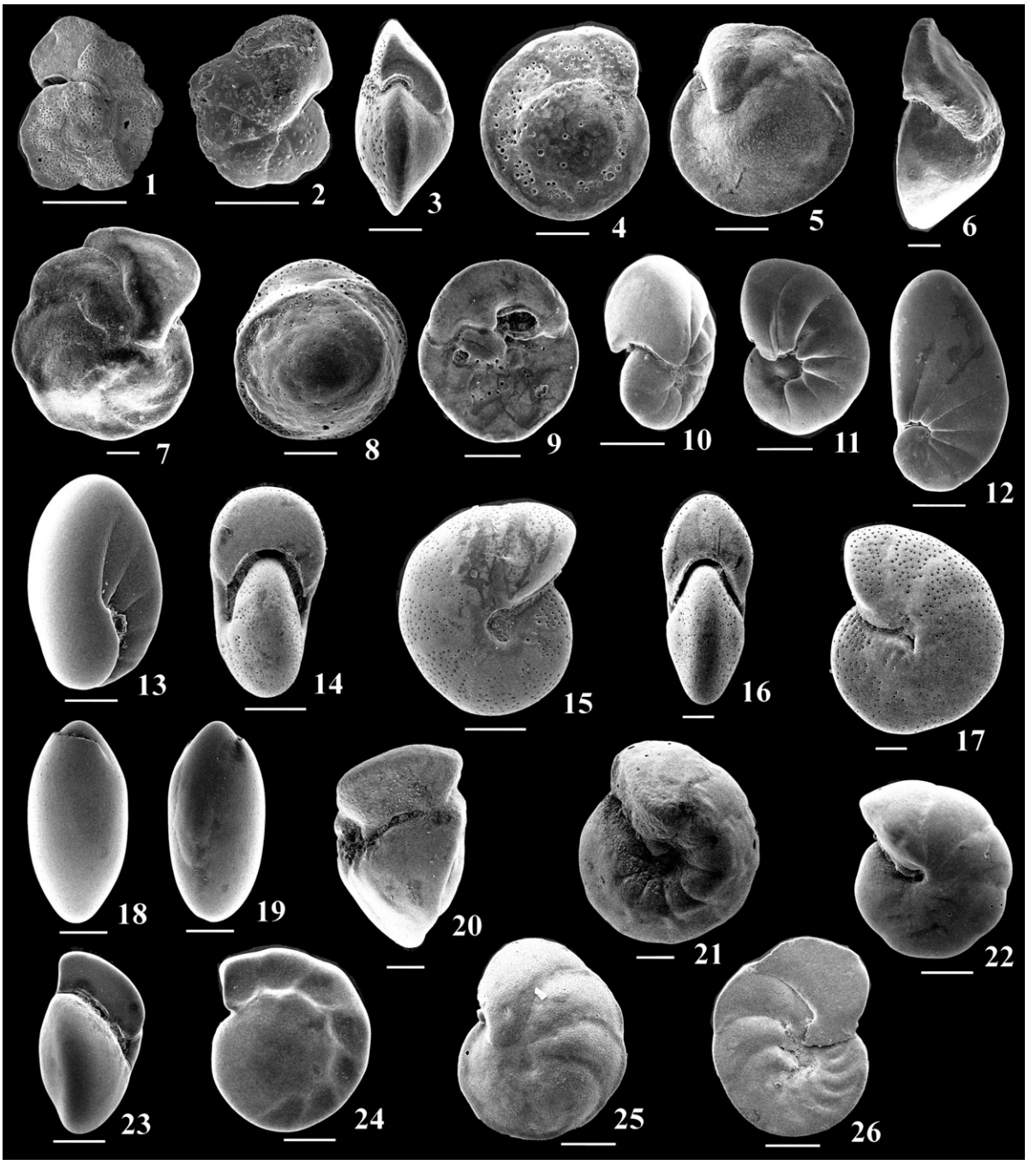

Plate III. 1–2, *Cibicides lobatulus* (Walker & Jacob): 1, spiral view; 2, umbilical view. 3–5, *Cibicides pachydermus* (Rzehak): 3, peripheral view; 4, spiral view; 5, umbilical view. 6–7, *Cibicides wuellerstorfi* (Schwager): 6, peripheral view; 7, umbilical view. 8–9, *Asterigerinata mamilla* (Williamson): 8, spiral view; 9, umbilical view. 10–11, *Nonion labradoricum* (Dawson): 10, apertural face view; 11, umbilical view. 12–13, *Nonionella turgida* (Williamson), umbilical views. 14–15, *Melonis affinis* (Reuss): 14, peripheral view; 15, umbilical view. 16–17, *Melonis barleeanum* (Williamson): 16, peripheral view; 17, umbilical view. 18–19, *Chilostomella mediterranensis* Cushman & Todd, peripheral views. 20–21, *Gyroidina altiformis* Stewart & Stewart: 20, peripheral view; 21, umbilical view. 22–24, *Gyroidina orbicularis* d'Orbigny: 22, umbilical view; 23, peripheral view; 24, spiral view. 25–26, *Hanzawaia boueana* (d'Orbigny): 25, umbilical view; 26, spiral view. Each scale bar represents 100 μm.

6.1. Core LC-31 (Levantine Basin, 2300 m depth)

In the entire pre-sapropel interval, to the onset of S1 at 10.4 ka BP, the *Miliolinella irregularis–Cibicides pachydermus* assemblage dominates (Fig. 4). *Quinqueloculina lamarckiana*, *Cassidulina carinata* and *Pyrgo murrhina* are also characteristic for this interval, whereas *Bulimina inflata*, *Uvigerina peregrina*, *Pyrgo lucernula* and *Articulina tubulosa* show rather discontinuous presence intervals. Total miliolids (includes all the miliolids species, see (Appendix B) represent about 60% of the fauna in this assemblage zone. The agglutinant taxon *G. charoides* is also present. The strong increase of *Spirophthalmidium acutimargo* at 17 ka BP is the most noteworthy faunal modification prior to 12.5 ka BP. Thereafter, *C. pachydermus* decreases gradually, reaching very low abundances around 13–11.5 ka BP. This event is accompanied by the total disappearance of *U. peregrina* and *B. inflata*, and by strong frequency decreases of *P. murrhina* and *C. carinata*. The 13–12 ka BP interval is characterized by a rapid repopulation by *C. pachydermus* that reaches a first interval of peak values. After a second total disappearance from 12–11.5 ka BP, coincident with the first appearance of *Gyroidina orbicularis*, *C. pachydermus* re-appears with a second relative frequency maximum between 11.5 and 10.5 ka BP. It disappears completely at the onset of S1 (Fig. 4). The lowest part of

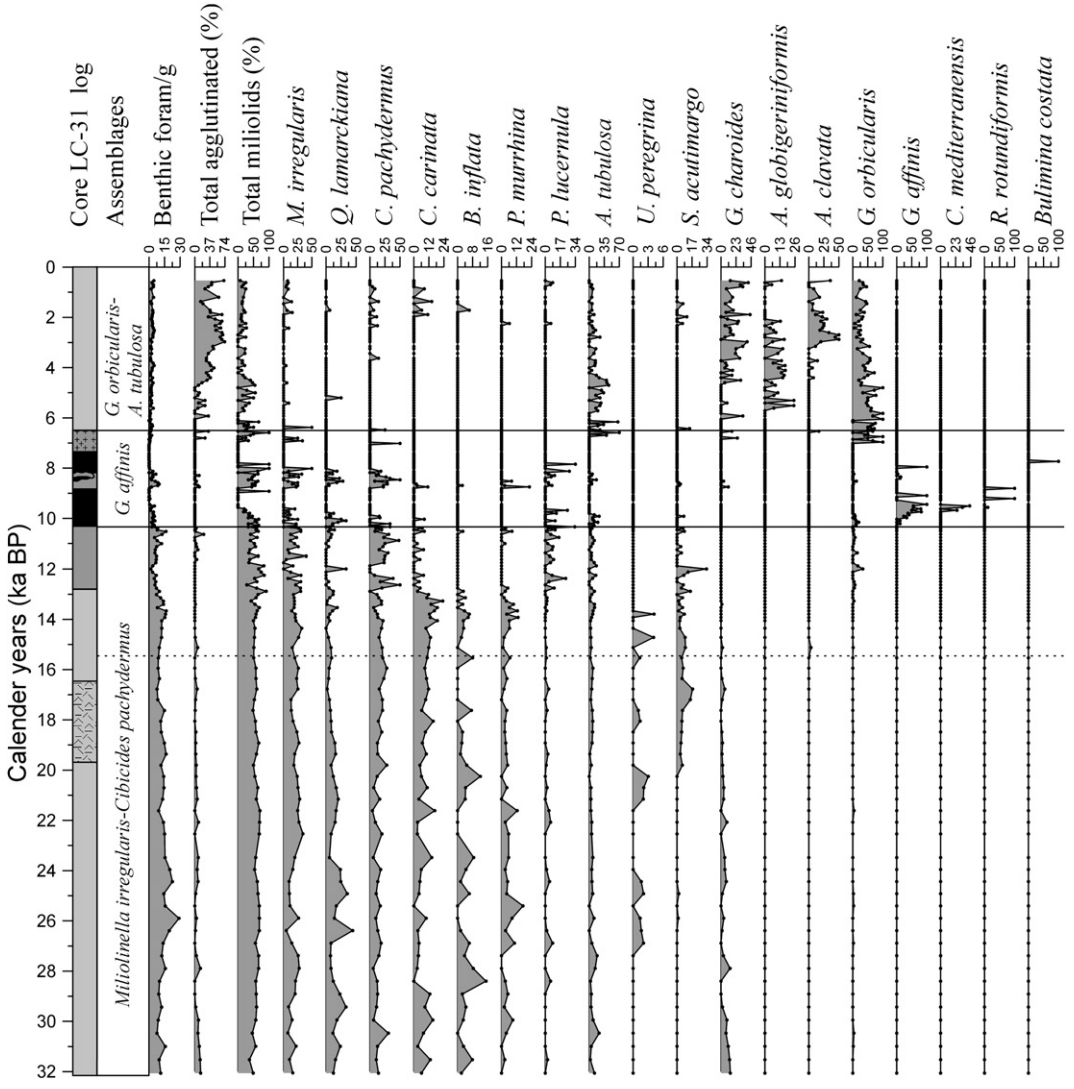

Fig. 4. Relative abundances of benthic foraminiferal species and the proposed faunal assemblages against calibrated AMS radiocarbon datings in core LC-31.

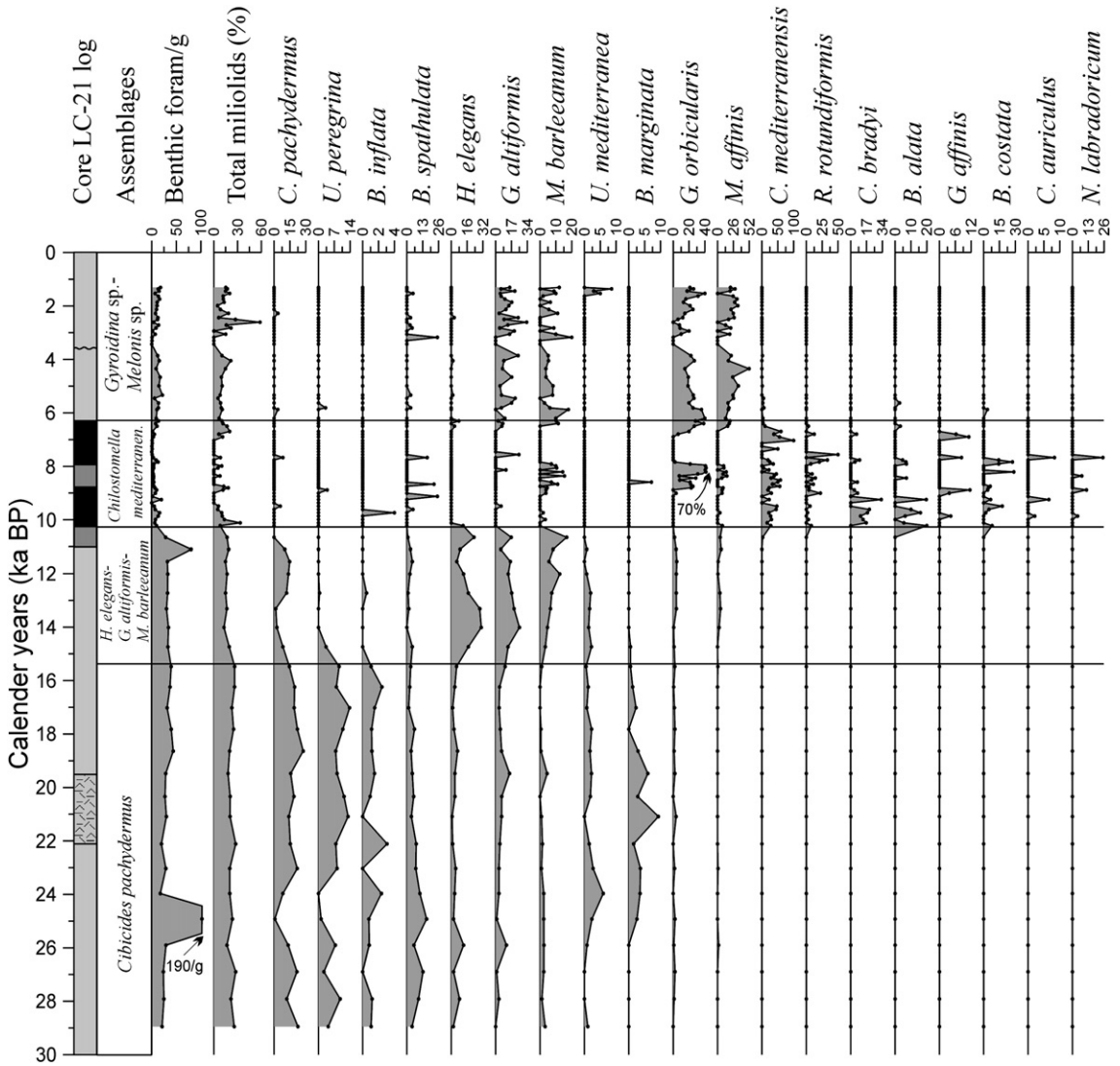

Fig. 5. Relative abundances of the most frequent benthic foraminiferal species and the proposed faunal assemblages against calibrated AMS radiocarbon datings in core LC-21.

the lithological S1 is characterized by high relative percentages of miliolids (especially *A. tubulosa*) and of *G. orbicularis* (Fig. 4).

The upper boundary of the *M. irregularis–C. pachydermus* assemblage zone is placed at the entry of the *G. affinis* assemblage at 10.4 ka BP, whereas all miliolid taxa exit at 9.6 ka BP (Fig. 4). The whole sapropel, except for the interruption interval, shows very low faunal density and diversity. There are sporadic appearances of *C. mediterranensis*, *Rutherfordoides rotundiformis* and *Bulimina costata*. Most of the species that are recorded below S1 re-appear in the small slump identified within the interruption interval in core LC31 (8.8–7.8 ka BP).

Following a brief (7 cm = ~700 years) interval above S1, which likely reflects a post-depositionally oxidised part of the sapropel (Fig. 4), the *G. orbicularis–A. tubulosa* assemblage starts at 6.8 ka BP. This assemblage dominates the entire post-sapropel interval. From ~5 ka BP to the Present, it is associated with high percentage of total agglutinated species such as *Rhabdammina abyssorum Psammosphaera fusca*, *Lagenammina laguncula*, *A. clavata*, *G. charoides*, *Reophax agglutinates*, *A. globigeriniformis* and *Trochamminopsis quadriloba* (Fig. 4). *G. charoides*, *A. clavata*, *A. globigeriniformis*, *R. abyssorum*, *P. fusca* and *L. laguncula* are the dominant ones (Fig. 4). The perforate

taxa *C. carinata* and *C. pachydermus* re-appear sporadically in the top ~2500 years of core (Fig. 4).

6.2. Core LC-21 (SE Aegean Sea, 1520 m depth)

The *C. pachydermus* assemblage dominates the interval from the base to 15.5 ka BP (Fig. 5). *U. peregrina*, *B. inflata*, *B. marginata*, *U. mediterranea*, *B. spathulata*, *B. albatrossi*, *Cibicides wuellerstorfi* and *C. carinata* are other important taxa (Figs. 5–6). Total miliolids show a fairly constant abundance throughout this interval, representing about 30% of the fauna (Fig. 5). The upper boundary of this assemblage is best defined at the exit of *U. peregrina*, *B. inflata* and *B. marginata*. Total sum of all miliolids (Appendix B) also decreases rapidly at 15.5 ka BP, to a relatively stable abundance level (15%) for the succeeding interval until S1 (Fig. 5). The 15.5 ka BP level marks the onset of the *Hoeglundina elegans–Gyroidina altiformis–Melonis barleeanum* assemblage. That assemblage dominates until 10.2 ka BP (Fig. 5). It starts with an increase until peak abundances are attained at 14–13 ka BP, followed by a remarkable decline around 12.5–11 ka BP (Younger Dryas). A second peak, below S1, ends in an abrupt disappearance with the onset of S1 (10.2 ka BP). *C. pachydermus*, which shows a gradual but marked decline centred at 14–13 ka BP, returns to form a broad peak which is more prominent at 12 ka BP (Younger Dryas), followed by an almost complete absence from the rest of the record (Fig. 5).

The *H. elegans–G. altiformis–M. barleeanum* assemblage disappears at the onset of S1 at 10.2 ka BP, where they are replaced by the *C. mediterranensis* assemblage. The *C. mediterranensis* assemblage first appears at 10.2 ka BP and dominates the S1 faunas (10.2–6.4 ka BP) (Fig. 5). *R. rotundiformis*, *Cassidulinoides bradyi*, *Bolivina alata*, *G. affinis* and *B. costata* are also characteristic, while *Bolivina seminuda*, *Nonion labradoricum*, *Cancris auriculus*, *Suggrunda eckisi* and *Bolivinita quadrilatera* occur sporadically in this interval (Fig. 5). None of these species occur outside S1. The *C. mediterranensis* assemblage continues through the (light-colored) interruption of S1 at 8.8 to 7.8 ka BP, but it is there associated with high abundances of *G. orbicularis*, *M. barleeanum*, and *Melonis affinis*, which rapidly repopulated this interval. Total miliolids totally disappear at two intervals within S1, namely at 9.5–9 ka BP and at 7.6–7 ka BP (Fig. 5).

The *C. mediterranensis* assemblage ends at the top of S1 at 6.2 ka BP. There, the *Gyroidina* spp.–*Melonis* spp. assemblage appears rapidly, dominating the entire post-sapropel interval (Fig. 5). It represents more than 50% of the total fauna of this interval. The *Gyroidina* spp.–*Melonis* spp. assemblage shows the highest abundance immediately above S1 and then decreases to a more or less stable abundance (~60%) that is maintained from ~5 ka BP to the Present. Total miliolids averages about 10% of the total fauna in this assemblage, with a single prominent peak at 2.5 ka BP. After the Santorini ash layer (3.8 ka BP), that is virtually devoid of benthic foraminifera, the top part of this assemblage zone (3.5 ka BP–Present) shows enrichment with the sum total (%) of the agglutinated forms (Appendix B). *G.*

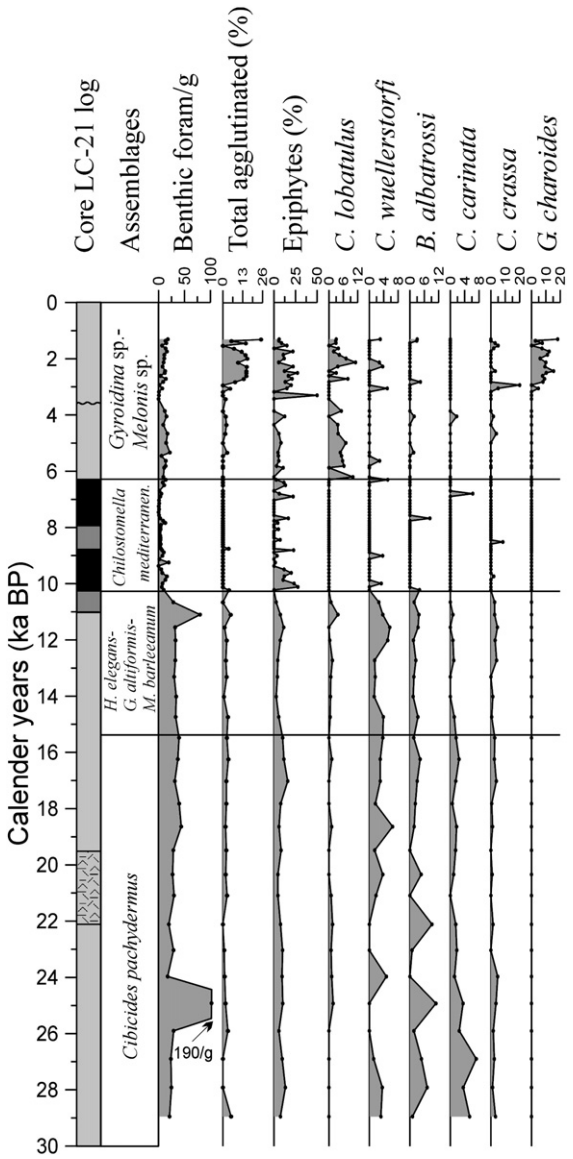

Fig. 6. Relative abundances of some common benthic foraminiferal species and the proposed faunal assemblages against calibrated AMS radiocarbon datings in core LC-21.

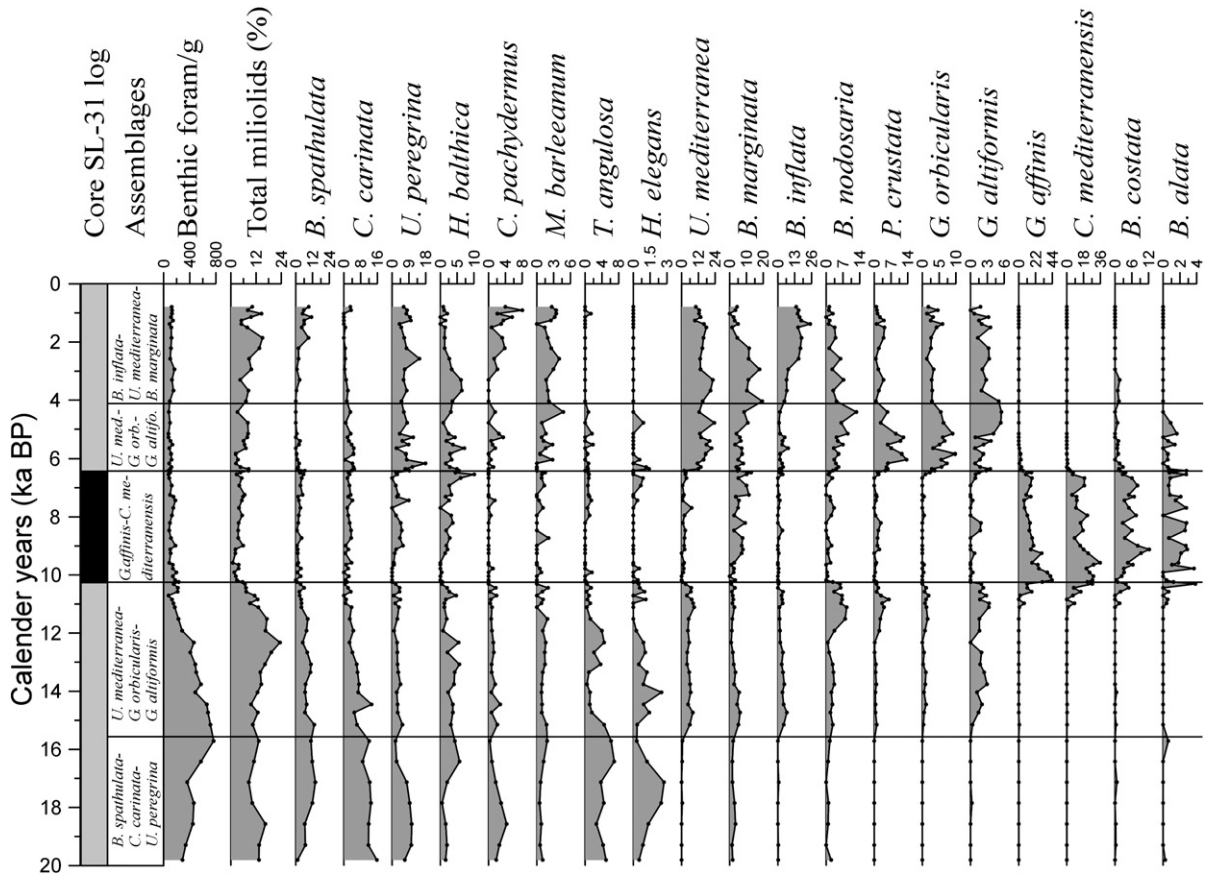

Fig. 7. Relative abundances of the most frequent benthic foraminiferal species and the proposed faunal assemblages against calibrated AMS radiocarbon datings in core SL-31.

charoides is the dominant species in this interval (Fig. 6). *U. mediterranea* re-appears at the top part of this interval, at about 1.5 ka BP (Fig. 5). The epiphytes (e.g. *Neoconorbina terquemi*, *Rosalina bradyi*, *Spirillina vivipara* and *Cornuspira planorbis*), *Robertina translucens*, *Cibicides lobatulus*, *S. acutimargo*, *M. subrotunda* and *M. irregularis* occur throughout this assemblage (Fig. 6).

6.3. Core SL-31 (Aegean Sea, 430 m depth)

The *B. spathulata–C. carinata–U. peregrina* assemblage dominates the interval from the base of the core to 15.5 ka BP (Fig. 7). At the upper boundary of this assemblage, species such as *C. pachydermus*, *Trifarina angulosa* and *C. carinata* show a decline in relative frequency, while species such as *Uvigerina mediterranea*, *B. marginata*, *B. inflata* and *Bigenerina nodosaria* show an increase (Fig. 7). The lower boundary of this assemblage does not appear in this study, while the upper boundary is best defined at the first entry of the *U. mediterranea–G. orbicularis–G. altiformis* assemblage which dominates the interval from 15.5 to 10.2 ka BP (Fig. 7).

The three main species in the *U. mediterranea–G. orbicularis–G. altiformis* assemblage, as well as *B. inflata*, *B. nodosaria*, *Pseudoclavulina crustata*, *Sigmoilopsis schlumbergeri* and *B. marginata*, start to increase at 15.5 ka BP, but show a strong abundance decrease (except *U. mediterranea*) between 13 and 11.7 ka BP. This interval (13–11.7 ka BP) in contrary is marked by relative abundance peaks in *T. angulosa* and the sum total (%) of miliolids and epiphytes (e.g. *Patellina corrugata*, *N. terquemi*, *R. bradyi*, *Planorbulina mediterrerranensis*, *A. mamilla* and *Astrononion stelligerum*) (Figs. 7–8). Following this interval, the assemblage shows another increase to high abundances, but now faunas are very similar to middle Holocene post-S1 faunas, with high relative frequencies of *U. mediterranea*, *B. nodosaria* and *G. altiformis*. The faunal assemblage declines abruptly from 10.7 ka BP towards the base of S1 (10.2 ka BP) (Fig. 7). This rapid

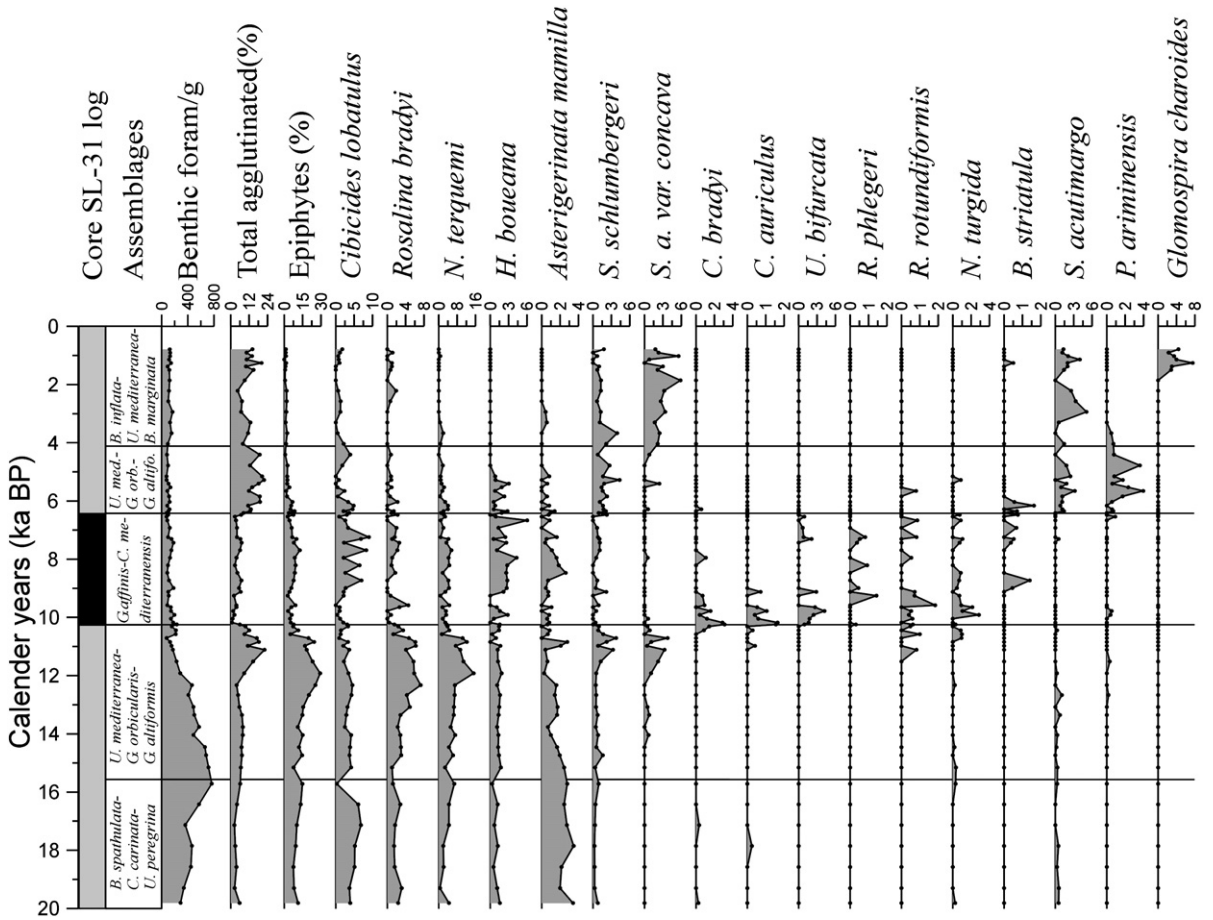

Fig. 8. Relative abundances of some common benthic foraminiferal species and the proposed faunal assemblages against calibrated AMS radiocarbon datings in core SL-31.

decline coincides with the first entry of the *G. affinis–C. mediterranensis* assemblage, which dominates through S1 from 10.2 to 6.4 ka BP (Fig. 7).

The *G. affinis–C. mediterranensis* assemblage is constrained to the interval immediately associated with S1, making its earliest appearance at 10.7 ka BP, and then increasing gradually in abundance to become the dominant assemblage by 10.2 ka BP (Fig. 7). Associated species are *C. bradyi*, *C. auriculus*, *Uvigerina bifurcata*, *B. costata*, *B. alata*, *Rectuvigerina phlegeri*, *Rutherfordiodes rotundiformis*, *Nonionella turgida* and *Bolivina striatula* (Figs. 7–8). In addition, several species that showed high abundances in the pre-sapropel interval remain present as minor constituents (e.g. *B. spathulata*, *C. carinata*, *U. peregrina*, *Hyalina balthica*, *B. marginata*, *U. mediterranea*, miliolids and epiphytic species) (Figs. 7–8). A rapid re-appearance and dominance of the *U. mediterranea–G. orbicularis–G. altiformis* assemblage at the end of S1 marks the end of the *G. affinis–C. mediterranensis* assemblage zone.

The *U. mediterranea–G. orbicularis–G. altiformis* assemblage, which was found previously in the interval immediately below S1, shows a second appearance in the interval after S1 from 6.4 to 4 ka BP, with associated high percentages of *B. nodosaria* (Fig. 7). Here, *U. mediterranea* becomes the most abundant species, achieving a more or less stable relative abundance that continues also after 4 ka BP. *B. nodosaria*, *S. schlumbergeri*, *U. peregrina* and *S. acutimargo* re-appear rapidly above S1 (Figs. 7–8). The resurgence of the *U. mediterranea–G. orbicularis–G. altiformis* assemblage ends at 4 ka BP with a strong increase of *B. inflata*, *B. marginata* and *C. pachydermus*, accompanied by a slight frequency decrease in *G. orbicularis*, *G. altiformis* and *B. nodosaria* to fairly constant relatively low abundances that continue to the core top (Fig. 7). *T. angulosa* and *H. elegans* disappear at this level (4 ka BP). *G. charoides* appears at ~2 ka BP, continuing to the top of the core (Fig. 8).

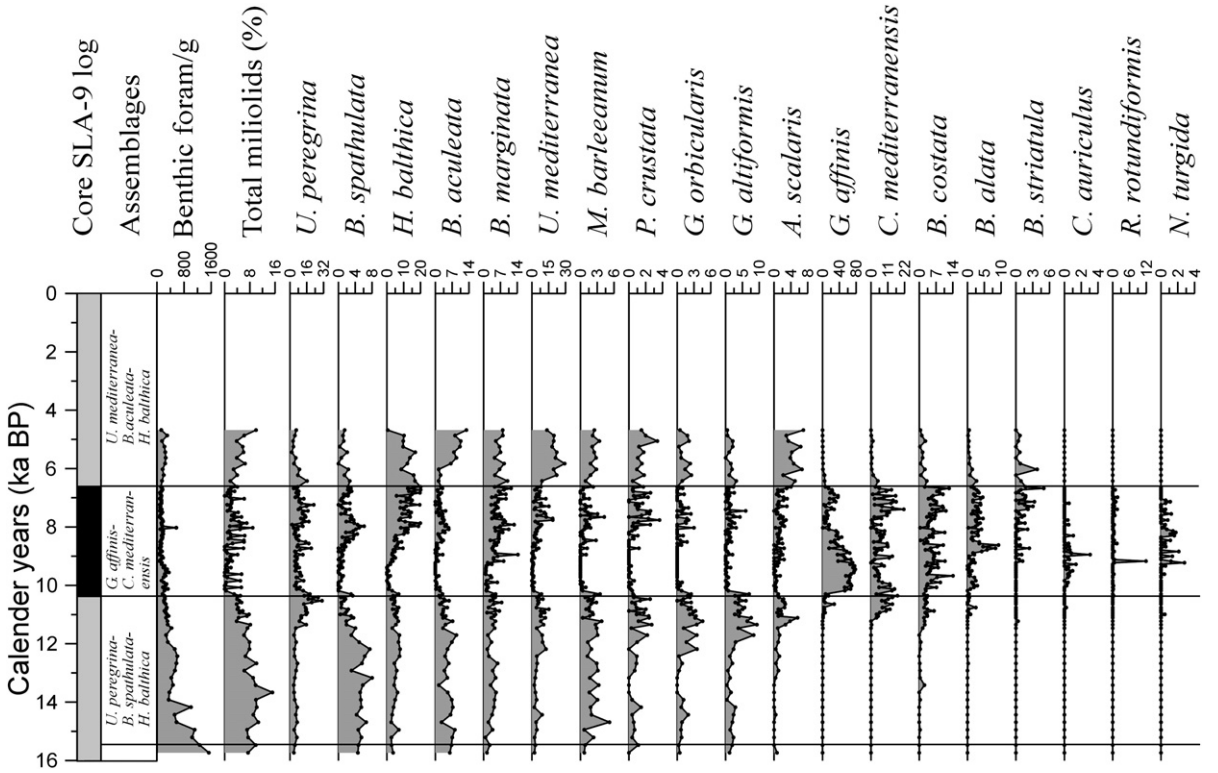

Fig. 9. Relative abundances of the most frequent benthic foraminiferal species and the proposed faunal assemblages against calibrated AMS radiocarbon datings in core SLA-9.

6.4. Core SLA-9 (Aegean Sea, 260 m depth)

The pre-sapropel interval from the base of the core to 10.4 ka BP is dominated by a *U. peregrina–B. spathulata–H. balthica* assemblage (Fig. 9), along with *C. carinata*, *T. angulosa*, *B. marginata*, *B. aculeata* and the sum total of the epiphytic forms such as: *P. corrugata*, *N. terquemi*, *R. bradyi*, *P. mediterrerranensis*, *Asterigerinata mamilla* and *A. stelligerum* (Figs. 9–10). At about 12 ka BP, *U. mediterranea*, *G. altiformis* and *G. orbicularis* show an important relative frequency increase. Immediately below S1, these species, together with *U. peregrina*, *Amphicoryna scalaris*, *P. crustata* and *B. nodosaria* show high relative abundances followed by rapid decreases that culminate in their almost total disappearance at 10.4 ka BP, in the lower part of S1 (Figs. 9–10).

The end of this assemblage has been defined at the first entry of *G. affinis–C. mediterranensis* assemblage that reaches about 80% of the total fauna around 10.4 ka BP (Fig. 9). The *G. affinis–C. mediterranensis* assemblage is mostly confined to S1, showing maximum frequency between 10.4 and 6.6 ka BP. *B. costata*, *B. alata*, *B. striatula*, *C. auriculus*, *R. rotundiformis* and *N. turgida* are other characteristic species for this assemblage (Fig. 9). *U. peregrina* and *B. marginata* occur throughout this assemblage in low abundances. Around 8 ka BP (sapropel "interruption"), the *G. affinis–C. mediterranensis* assemblage is enriched with faunal elements that characterized the preceding (pre-sapropel) assemblage. The *G. affinis–C. mediterranensis* assemblage zone ends at the upper boundary of S1 (6.6 ka BP). At that level, the *U. mediterranea–B. aculeata–H. balthica assemblage* rapidly gains dominance, prevailing over the post-S1 interval (Fig. 9). The faunal composition of this assemblage is very similar to that in the interval immediately below S1, except that miliolids and epiphytes remain less abundant (Figs. 9–10).

7. Discussion

The interpretation of our faunal record is largely based on a combination of numerous papers describing foraminiferal microhabitats and ecology of the dominant taxa, as extensively discussed in (Jorissen, 1999a, 1999b) and Jorissen et al. (2007). In accordance to the ideas expressed in these papers, most trochospiral, sediment-surface-dwelling ("epifaunal") species are considered

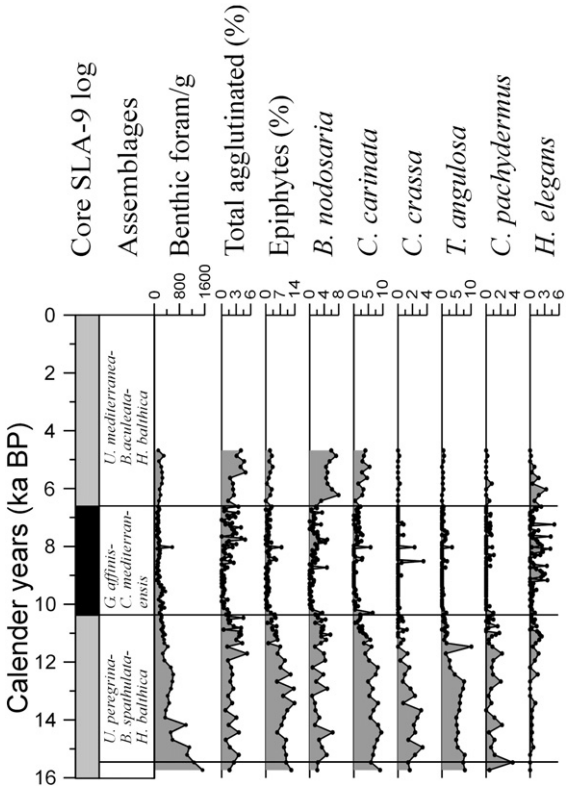

Fig. 10. Relative abundances of some common benthic foraminiferal species and the proposed faunal assemblages against calibrated AMS radiocarbon datings in core SLA-9.

"opportunistic" (e.g. Gooday, 1988) in that such species can react to a sudden input of high-quality (labile) organic matter, by enhanced reproductive activity and/or rapid growth. Over the past few years, an increasing amount of information has become available that shows such a response for trochospiral taxa such as *Epistominella exigua* (e.g. Gooday, 1988; Gooday and Turley, 1990; Jannink et al., 1998; Fontanier et al., 2003), *Gyroidina* spp., *Cibicidoides* spp. and *C. carinata* (Jorissen and Wittling, 1999). However, it is evident that such opportunistic taxa are not restricted to eutrophic ecosystems. Also in very oligotrophic conditions, episodic phytodetritus inputs can lead to an opportunistic response of some adapted species, as exemplified by the reproductive response of *E. exigua* to a phytodetritus deposit at 4800 m depth (Gooday, 1988). In practice, highly intermittent supplies of organic matter can be found in eutrophic, mesotrophic, and oligotrophic ecosystems. However, the opportunistic species responding to the sudden organic supplies will not be the same; a comparison of their recent distribution (De Rijk et al., 1999b, 2000) and their occurrence in our cores suggest that *C. pachydermus* and *C. carinata* are the most important opportunistic species in eutrophic conditions in the Mediterranean. In more mesotrophic environments they are replaced by *H. elegans*, whereas towards more oligotrophic ecosystems, they are replaced first by *G. altiformis*, and finally by *G. orbicularis*.

Because of their high densities in eutrophic areas, many biserial and triserial shallow-infaunal taxa, belonging to the genera *Bolivina*, *Bulimina* and *Uvigerina*, are often systematically considered as opportunistic taxa. However, the fact that these taxa are less restricted to the sediment surface than many trochospiral taxa, suggests that they are more dependent on a rather continuous abundance of organic matter, eventually of a lower quality. There is a fundamental difference between "eutrophic" and "opportunistic" taxa. Because of their dominance in eutrophic ecosystems, and their general absence in more oligotrophic systems, many of the aforementioned biserial and triserial taxa do qualify for the first adjective, but cannot be systematically considered as opportunists.

7.1. From the base of the cores to 15.5 ka BP

This interval displays the highest absolute benthic foraminiferal abundances in all cores. It is generally accepted that large standing stocks are related to the abundance of food, while low standing stocks reflect low levels of food within the deep-sea environment (e.g. Thiel, 1983; Altenbach and Sarnthein, 1989; Bernhard, 1992). Herguera and Berger (1991) empirically related surface productivity to the rate of benthic foraminiferal accumulation on the sea floor, suggesting that for each 1 mg of organic carbon arriving at the sea floor per square centimeter, one benthic foraminiferal shell >150 μm is deposited. Although we cannot exclude that the foraminiferal densities per gram dry weight are to some extent affected by differences in the sediment accumulation rates, the much higher densities at shallower sites (SL-31, SLA-9) than at deep sites (LC-21 and LC-31) still suggest a higher organic flux to the sea floor at the shallower sites than at the deep sites, during the deposition of this interval. Moreover, the observation that foraminiferal densities are much higher in this interval than in the top sections of all four cores suggests that export production at glacial times was considerably higher than today.

These notions are corroborated by the relative abundance patterns of individual taxa. In the deeper cores (LC-31 and LC-21), the pre-15.5 ka BP interval is dominated by *C. pachydermus*, sum total of the miliolid taxa (the dominant ones are *M. irregularis*, *Quiqueloculina*

lamarckiana and *A. tubulosa*), *B. spathulata*, *C. carinata*, and *U. peregrina*. Today, these taxa occupy epifaunal or shallow-infaunal microhabitats, restricted to the top 1 or 2 cm of the sediment (Corliss, 1991; De Stigter et al., 1998; Mackensen and Douglas, 1989). In core LC31 (2300 m), the strong dominance of these superficially-living taxa nevertheless suggests a food-limited, rather oligotrophic environment with high bottom-water oxygen concentration values. The fluctuating, but sometimes very high, percentages of the more opportunistic species *C. pachydermus* and *C. carinata* suggest that a major part of the organic flux to the sea floor was due to intermittent (seasonal and/or interannual) surface-water bloom events and subsequent phytodetritus deposits. The low but repetitive percentage peaks of the shallow-infaunal taxa *B. inflata* and *U. peregrina* suggest periodical development of a microhabitat succession that reflects more mesotrophic conditions with a more constant organic flux to the sea floor. In core LC-21 (1500 m), the about 3 times higher foraminiferal densities, much lower proportion of miliolids, and permanent presence of shallow-infaunal taxa (*B. spathulata*, *U. peregrina* and *B. marginata*), combine to suggest an environment with a definitely higher organic flux than at the site of LC31. Still, elevated percentages of *C. pachydermus* suggest that a significant part of the organic flux occurred in intermittent events. As in LC31, the virtual absence of deep infaunal elements indicates a well-oxygenated benthic ecosystem.

B. spathulata, *U. peregrina*, *C. carinata*, *C. pachydermus*, and *H. balthica*, together with *T. angulosa*, are also characteristic for the pre-15.5 ka BP interval in the much shallower cores SL-31 (450 m) and SLA-9 (260 m). This combination of epifaunal and shallow-infaunal taxa is today found in relatively eutrophic ecosystems with a well-oxygenated sediment–water interface (Barmawidjaja et al., 1992; De Stigter et al., 1998; Corliss and Chen, 1988; Morigi et al., 2001). The dominance of this group in the shallow Aegean Sea testifies of the eutrophic nature of this basin in glacial times. Relatively low (in comparison to the deeper cores) percentages of the more opportunistic superficially-living taxa *C. pachydermus* and *C. carinata* may suggest that the benthic ecosystem relied on continuous rather than episodic supply of organic matter to the sea floor. The total absence of deep infaunal taxa is indicative of well-oxygenated bottom waters, despite the relatively eutrophic context at this shallow site.

Our interpretation of the glacial faunas is corroborated by the surface-water reconstruction based on planktonic foraminiferal faunas of Casford et al. (2002). That study (based on the same cores) shows that the planktonic foraminiferal faunas consisted mainly of cool/eutrophic water indicators such as *Neogloboquadrina pachyderma* and *Turborotalia quinqueloba*, with an absence of warm epipelagic, more oligotrophic species (e.g. *Globigerinoides ruber*). The $\delta^{18}O$ values of both epipelagic *G. ruber* (white) and mesopelagic *N. pachyderma* (right-coiling) were found to be much (about 3‰) heavier than core-top values, and relatively close together, throughout the whole pre-sapropel interval, indicating a homogenized, cool and/or salty water column. Cool/salty surface conditions and a well-mixed water column together are suggestive of enhanced deep-water ventilation, while generally eutrophic conditions in the surface waters as indicated by the dominance of *N. pachyderma* and *T. quinqueloba* would be conducive to a good supply of high-quality food (labile organic matter) to the benthic ecosystem.

7.2. From 15.5 to 10.2 ka BP

Remarkable faunal changes can be observed in this interval. In core LC-21 (1500 m), *H. elegans*, *G. altiformis* and *M. barleeanum* become dominant around 15.5 ka BP, following an abrupt decline in the shallow-infaunal triserial taxa *U. peregrina*, *B. inflata*, and *B. marginata*, which indicates a virtually complete closure of shallow-infaunal niches (only minor quantities of *U. mediterranea* and *B. spathulata* persist). This faunal pattern suggests a significant decrease of trophic resources. At the sediment surface, *C. pachydermus* is gradually replaced by *H. elegans* and *G. altiformis*, taxa that may also have an opportunistic tendency but are characteristic of poorer environments. This corroborates the inferred reduction of food supply to the sea floor at this time. Further support comes from the appearance of important amounts of *M. barleeanum*, which is indicative of an intensive occupation of intermediate infaunal microhabitats (e.g. Corliss, 1991; Mackensen et al., 2000). In eutrophic ecosystems (such as found before 15.5 ka), the oxygenated layer of the sediment is normally very shallow (1 cm or less). As a consequence, the successive microhabitat zones are strongly compressed, and show important overlaps, which leads to poor development of the intermediate infaunal niche (Fontanier et al., 2002). With a decreasing organic input, the oxygenated layer expands, so that a wider range of microhabitat zones becomes established. Under such oligotrophic conditions, intermediate infaunal taxa (here represented by *M. barleeanum*) may become very successful (Jorissen et al., 1995; Fontanier et al., 2002).

The much shallower core SL-31 (450 m) also shows important faunal changes around 15.5 ka BP: *U. mediterranea*, *B. inflata*, *G. orbicularis*, *G. altiformis*

and *B. nodosaria* simultaneously rapidly increase and become more dominant, while species such as *B. spathulata*, *C. carinata*, and *T. angulosa* show a relative decrease. Since the newly appearing taxa are all indicative of mesotrophic or even oligotrophic (*G. orbicularis*) conditions, whereas the decreasing taxa are all typical of more eutrophic conditions, this faunal change around 15.5 ka BP in SL-31 likely reflects a significant decrease in organic flux to the sea floor, similar to that noted in core LC-21.

Between 13 and 10.2 ka BP, there are several rapid faunal changes in our cores. A general trend of impoverishment of the sea floor is reflected by: (1) the strongly decreasing foraminiferal densities in all cores except LC-21; and (2) the total disappearance of shallow-infaunal taxa (*B. inflata* and *U. peregrina*) in core LC-31 (2300 m), and increasing abundances of more mesotrophic taxa in core LC-21 (*G. altiformis*, *H. elegans* and *M. barleeanum*) and core SL-31 (*U. mediterranea*, *B. nodosaria* and *P. crustata*) at the expense of the preceding eutrophic faunas. However, this trend towards more oligotrophic conditions is interrupted by an abrupt return to more eutrophic conditions with intermittent supply of organic matter to the sea floor, during the Younger Dryas (12.8–11.5 ka BP). In cores LC-31 (2300 m) and LC-21 (1500 m), this is revealed by a strong peak of *C. pachydermus*, while core SL-31 (450 m) shows a return of high abundances of miliolids and *T. angulosa*. Only core SLA-9 (260 m), which on account of its shallow water depth shows eutrophic conditions throughout, does not reveal a distinct eutrophication increase during the Younger Dryas. It does, however, show a shift to less eutrophic conditions immediately after the Younger Dryas, at 11.5 ka BP, in the form of an increase in the oligotrophic taxa *G. altiformis* and *G. orbicularis* that are common in deep-water settings (De Rijk et al., 2000).

A similar shift to more oligotrophic conditions at 11.5–10.2 ka BP, following the Younger Dryas and immediately preceding sapropel S1, is seen in the other cores. In core LC-21 (1500 m), *C. pachydermus* disappears around 10.8 ka BP, some 500 years before the strong increase of deep infaunal taxa that is typical of the onset of low-oxygen conditions. The disappearance of *C. pachydermus* coincides with the return of a more oligotrophic fauna dominated by *H. elegans*, *G. altiformis*, and *M. barleeanum*. In core SL-31, the 11.5–10.2 ka BP interval is represented by low density faunas with abundant *U. mediterranea*, *G. altiformis*, *B. nodosaria*, and *P. crustata*, which are similar to both the Late Holocene and core-top faunas at this site.

The observed shift to more oligotrophic conditions at the sea floor during the ~1000 years between the end of the Younger Dryas and the onset of S1 indicates that sapropel formation in the Aegean and NE Levantine region studied here cannot be ascribed to a culmination of a long-term eutrophication trend. That inference was made previously for an Adriatic Sea sequence into sapropel S1 (Rohling et al., 1997), but it should be noted that S1 in that basin started only around un-calibrated 8.3 ka BP (see also Mercone et al., 2000), following a trend of increasing sea-floor eutrophication that started since about un-calibrated 9.3 ka BP (Rohling et al., 1997). It would appear that S1 formation started in the Aegean/NE Levantine sector at the same time as the shift to more eutrophic conditions in the Adriatic Sea, roughly at 10.2 ka BP, and that it took another 1000 years before sapropel deposition commenced in the Adriatic Sea. We infer that the difference in the timing of the S1 onset between the two regions resulted from differences in deep-water ventilation (oxygen advection); apparently, deep ventilation was a more robust process in the Adriatic than in the rest of the eastern Mediterranean (likely due to stronger regional winter cooling; see also circulation models by Myers et al., 1998).

7.3. From 10.2 to 6.4 ka BP

In this interval, all benthic foraminiferal taxa recorded before are replaced by new arrivals, such as *C. mediterranensis*, *G. affinis*, *R. rotundiformis*, *C. bradyi*, *B. alata* and *B. costata*. Today, these species are found abundantly under low-oxygen levels in sediments highly enriched in organic matter (Boltovskoy and Wright, 1976; Corliss, 1985; Corliss and Chen, 1988; Alavi, 1988; Corliss, 1991; Nolet and Corliss, 1990; De Stigter et al., 1998; Jorissen, 1999a; De Rijk et. al, 1999b). *G. affinis* and *C. mediterranensis* are frequently found in deep and intermediate-deep infaunal microhabitats, respectively, and are common in strongly oxygen-depleted or even anoxic sediments (e.g. Mackensen and Douglas, 1989; Corliss and Emerson, 1990; Bernhard and Reimers, 1991; De Stigter et al., 1998). In view of their exceptional tolerance of oxygen deficiency, and their appearance and strong abundance increase in the first centimeters of many sapropels, often followed by a rapid disappearance, their abundance patterns can be used to trace the onset of anoxic conditions (see also Rohling et al., 1997).

In core LC-31 (2300 m), some 1300 years elapse between the appearance of *G. affinis*(10.3 ka BP), its abundance maximum (9.8 ka BP), and its disappearance (9.0 ka BP). In core LC-21 (1500 m), some 600 years elapse between the arrival of *C. mediterranensis*

(10.2 ka BP) and the total disappearance of miliolids (9.6 ka BP). Apparently the change from well ventilated to strongly dysoxic bottom-water conditions took 500 to 600 years at these sites.

In the much shallower Aegean cores SL-31 (430 m) and SLA-9 (260 m), benthic foraminiferal faunas continue throughout sapropel S1. These faunas nearly always contain less low-oxygen resistant epifaunal and shallow-infaunal taxa, which indicates that long-term (more than several decennia) anoxia never developed at these sites. Still, a strong dominance of deep infaunal taxa suggests that the sea floor was generally very poorly oxygenated, and the presence of less low-oxygen tolerant taxa is likely to reflect exceptional, short-term re-ventilation events. These re-ventilation events that occurred during S1, were also indicated by Casford et al. (2003) through several sapropels from the western Levantine Basin and Aegean cores.

The above shows that highly restricted to (periodically) inhibited bottom-water ventilation prevailed throughout S1 formation. Between about 9 and 8 ka BP, we note evidence of marked re-oxygenation. In core LC-31, a small slump unfortunately compromises this interval with the same benthic foraminiferal species recorded in the glacial interval (below S1), precluding any conclusions from our deepest site. In core LC-21, on the contrary, the re-ventilation interval is intact, and characterized by unprecedented faunas with particularly high abundances of *G. orbicularis*. Note that this species is an indicator for the oligotrophic conditions that characterize Late Holocene faunas at this site. In the shallow cores SL-31 and SL-9, the re-ventilation interval is characterized by a significant abundance decrease of the species that dominate the sapropel intervals.

Our inference of reduced bottom-water ventilation during S1 formation is corroborated by changes in the $\delta^{13}C$ values of both benthic and planktonic foraminiferal species (Casford et al., 2003). The $\delta^{13}C$ of benthic foraminifera (*G. affinis*, *C. mediterranensis*, *B. marginata* and *U. peregrina*) and *N. pachyderma* (a deep dwelling planktonic foraminiferal species) was found to show a much stronger shift to lighter values than the $\delta^{13}C$ of the surface-dwelling planktonic species *G. ruber*, suggesting enhanced subsurface accumulation of ^{12}C from respiration in deep and intermediate waters due to reduced deep-water ventilation.

7.4. From 6.4 ka BP to the Present

Immediately above S1, faunas appear that virtually lack the deep infaunal taxa that dominated the sapropel. In the deep cores LC-31 and LC-21, where an important part of the sapropelic sediment is devoid of benthic faunas, the first recolonizing faunas consist of miliolids (abundant *A. tubulosa*) and *Gyroidina* species. As these colonizing taxa have very limited resistance to low-oxygen conditions, it is clear that a very rapid re-oxygenation of the benthic ecosystem terminated the deposition of sapropel S1. This strongly suggests that the termination of sapropel deposition was due to an abrupt onset of efficient, convective deep-water ventilation.

In core LC-31 (2300 m) *G. orbicularis* is the first species to recolonize the sea floor after S1, and it then continues to dominate the low density Holocene faunas, together with miliolid taxa. Agglutinated taxa (*G. charoides*, *A. globigeriniformis* and *A. clavata*) appear around 5.0 ka BP. These early post-S1 faunas are typical for the very oligotrophic faunas found in the Levantine Basin today (Parker, 1958; De Rijk et al., 2000). Traces of more opportunistic superficial taxa (*C. pachydermus* and *C. carinata*) appear around 2.5 ka BP, and suggest slight ecosystem enrichment.

In core LC-21 (1500 m), *G. orbicularis*is quickly followed by *G. altiformis*, as well as the intermediate infaunal taxa *M. affinis* and *M. barleeanum*. The post-S1 Holocene faunas (absolute density) at this site are much poorer than the glacial faunas, but the presence of abundant intermediate infaunal taxa in the Holocene of LC-21 attests to a generally higher organic flux than at the site of LC-31. This likely reflects the difference in water depth (De Rijk et al., 2000). In LC-21, the agglutinant taxon *G. charoides* arrives around 2.5 ka BP.

In the shallower Aegean cores SL-31 and SLA-9, the Holocene faunas again reflect a significantly reduced trophic level relative to glacial faunas. Since sapropel S1 in the shallow Aegean cores contains benthic foraminifera throughout, the transition from sapropel to non-sapropel faunas is more gradual than in the deep cores LC-31 and LC-21. Deep infaunal taxa decrease gradually, being progressively replaced by a mixture of epifaunal and shallow-infaunal elements.

In core SL-31 (430 m) *U. mediterranea*, *U. peregrina*, *Hyalinea balthica*, *B. nodosaria*, *G. orbicularis* and *G. altiformis* dominate the repopulating faunas. At about 4.0 ka BP, the latter three species show a relative abundance decrease, the overall foraminiferal density increases, and *B. marginata*, *B. inflata*, *M. barleeanum* and *C. pachydermus* show strong increases. These changes suggest a progressive increase of trophic level over the last 4000 years of the core.

In core SLA-9 (260 m), which is truncated at about 5.0 ka BP, the post-sapropel faunas also show a steady increase of foraminiferal numbers. The initial post-sapropel faunal compositions are more or less the same

as in the upper half of S1 dominated by *Hyalinea balthica* (15%), *U. peregrina* (8%), *U. mediterranea* (7%), *B. marginata* (6%) and the deep infaunal taxa that dominated the sapropel. At 6.4 ka BP, *U. mediterranea*, *Bulimina aculeata*, *A. scalaris*, *B. nodosaria* and *C. carinata* show rapid abundance increases, whereas the deep infaunal taxa rapidly disappear. These faunal changes seem to be indicative of a rapid return to normal oxygenation and food supply. Moreover, the planktonic foraminiferal species *Globorotalia inflata* in this core and SL-31 returns abruptly at the end of S1, with a sharp abundance peak at ~6.5 ka BP that likely reflects vertical mixing of the water column associated with the rapid bottom-water re-ventilation (Casford et al., 2002). Thereafter, *G. inflata* decreases gradually to a disappearance around 4.0 ka BP.

All our cores show that the end of S1 was characterized by a rapid re-establishment of sediment-surface-dwelling taxa that have only limited tolerance to low-oxygen conditions. This indicates that bottom-water oxygenation was established very rapidly.

The delayed appearance of many of the agglutinant taxa (such as *G. charoides*) most probably is an artifact. Most agglutinant taxa have a chitinous cement that disintegrates with time, and their restriction to the very top of the cores likely reflects the disintegration of agglutinated tests during diagenetic processes (Bizon and Bizon, 1984a). The exception is the occurrence of *G. charoides* in the interval below 15.5 ka BP of Core LC-31. This is could be related to the presence of better preservation conditions or low microbial activity (Edelman-Furstenberg et al., 2001).

8. Conclusions

Our cores indicate that, at all times within the studied intervals, there was trophic gradient from the shallow sites with a relatively high organic flux to the sea floor, to the deep sites with a much lower flux. All four cores show a gradual decrease in trophic level at the sea floor from LGM times to about 10.2 ka BP, characterized by a steady decrease of foraminiferal density and the replacement of certain species by more oligotrophic counterparts. However, this overall decrease is interrupted by a short-term return to more productive conditions during the Younger Dryas (12.8–11.5 ka BP). Faunas immediately preceding the sapropel (11.5–10.2 ka BP) are characterized by an increase in the relative abundances of more oligotrophic species, which dominate the post-sapropel faunas. The presence of rather oligotrophic conditions directly before deposition of the sapropels rules out the possibility of a long-term (several thousand years) eutrophication culminating in sapropel deposition.

From the base of the studied records to about ~10.2 ka BP, deep-waters were well ventilated throughout. The strong decrease of bottom-water oxygenation, culminating in total anoxia at the onset of S1, took about 600 years. From 10.2 to 6.4 ka BP, anoxic conditions prevailed in the Levantine Basin, while the shallower Aegean sites were characterized by severely dysoxic conditions that were interrupted by intermittent re-oxygenation events. Re-ventilation of the bottom waters at the end of S1 was extremely rapid, and Late Holocene faunas suggest a much lower organic flux regime than during glacial times.

Acknowledgements

This work is part of RHAZ's 1997–2001 PhD project at Southampton, which was generously funded by the Egyptian Government. This study contributes to NERC project NER/B/S/2002/00268. We thank A. Kemp and R. Pearce for their help in obtaining the SEM images for the studied foraminifera, John Murray and Andy Gooday for their support, suggestions, and assistance, and V. Lykousis for organizing and coordinating the Aegean coring aboard *R.V. Aegeo*.

Appendix A. Benthic foraminiferal species list

Psammosphaera fusca Schulze, 1875–Jones (1994), p. 31, pl. 18, figs. 1–8.

Rhabdammina abyssorum M. Sars, 1869–Jones (1994), p. 32, pl. 21, figs. 1–8, 10–13.

Rhabdammina discreta Brady, 1881–Jones (1994), p. 32, pl. 22, figs. 7–10.

Lagenammina laguncula Rhumbler, 1911–Loeblich and Tappan (1987), p. 31, pl. 21, fig. 9.

Ammolagena clavata (Jones and Parker, 1860)–Cita and Zocchi (1978), pl. 3, fig. 4.

Glomospira charoides (Jones and Parker, 1860)–Bizon and Bizon (1984b), pl. IV, figs. 1–4.

Reophax agglutinatus Cushman, 1913–Cushman (1932), p. 4, pl. 1, figs. 1–3.

Ammoglobigerina globigeriniformis (Parker and Jones, 1865)–Loeblich and Tappan (1987), p. 126, pl. 128, figs. 9–10.

Trochamminopsis quadriloba (Höglund, 1948)–Loeblich and Tappan (1987), p. 122, pl. 129, figs. 1–3.

Bigenerina nodosaria d'Orbigny, 1826–Ayyad et al. (1991), pl. 1, fig. 1.

Pseudoclavulina crustata Cushman, 1936–Jorissen (1988), pl. 1, fig. 1.

Spirillina vivipara Ehrenberg, 1841–Parker (1958), p. 264, pl. 3, fig. 4.

Patellina corrugata Williamson, 1858–Jones (1994), p. 93, pl. 86, figs. 1–7.

Cornuspira planorbis Schultze, 1854–Loeblich and Tappan (1987), p. 310, pl. 322, figs. 7–8.

Spirophthalmidium acutimargo (Brady, 1884)–Loeblich and Tappan (1987), p. 327, pl. 334, figs. 10–11.

Spirophthalmidium acutimargo concava Heron-Allen and Earland, 1916–Lander Rasmussen (1991), p. 376, fig. 6 (1).

Quinqueloculina lamarckiana d'Orbigny, 1839–Lankford and Phleger (1973), p. 126, pl. 1, fig. 23.

Miliolinella irregularis (d'Orbigny, 1839)–Lander Rasmussen (1991), p. 376, fig. 6 (3).

Miliolinella subrotunda (Montagu, 1803)–Loeblich and Tappan (1987), p. 340, pl. 350, figs. 1–12.

Pyrgo lucernula (Schwager, 1866)–Mullineaux and Lohmann (1981), p. 38, pl. 1, figs. 14–15.

Pyrgo murrhina (Schwager, 1866)–Mullineaux and Lohmann (1981), p. 38, pl. 1, fig. 13.

Sigmoilopsis schlumbergeri (Silvestri, 1904)–Jorissen (1988), pl. 4, fig. 9.

Articulina tubulosa (Seguenza, 1862)–Parker (1958), p. 255, pl. 1, figs. 12–13, 18–19.

Amphicoryna scalaris (Batsch, 1798)–Cita and Zocchi (1978), pl. 1, fig. 2.

Hoeglundina elegans (d'Orbigny, 1826)–Lohmann (1978), p. 29, pl. 4, figs. 10–11.

Robertina translucens Cushman and Parker, 1936–Parker (1958), p. 263, pl. 2, fig. 34.

Bolivina alata Seguenza, 1862–Wright (1978), p. 710, pl. 1, fig. 13.

Bolivina albatrossi Cushman, 1922–Wright (1978), p. 710, pl. 1, figs. 14–15.

Bolivina seminuda Cushman, 1911–Barmawidjaja et al. (1992), pl. 2, figs. 1–4.

Bolivina spathulata (Williamson, 1858)–Lander Rasmussen (1991), p. 376, fig. 6 (12).

Bolivina striatula (Cushman, 1922)–Barmawidjaja et al. (1992), pl. 2, figs. 10–13.

Bolivinita quadrilatera (Schwager, 1866)–Loeblich and Tappan (1987), p. 503, pl. 554, figs. 6–10.

Cassidulina carinata Silvestri, 1896–Ross and Kennett (1984), pl. 1, figs. 14–15.

Cassidulina crassa d'Orbigny, 1839–Phleger et al. (1953), p. 44, pl. 10, fig. 1.

Cassidulinoides bradyi (Norman, 1881)–Jones (1994), p. 60, pl. 54, figs. 6–9.

Bulimina aculeata d'Orbigny, 1826–Jorissen (1987), p. 46, pl. 4, fig. 5.

Bulimina costata d'Orbigny, 1826–Jorissen (1988), pl. 1, fig. 9.

Bulimina inflata Seguenza, 1862–Wright (1978), p. 712, pl. 3, figs. 8–9.

Bulimina marginata d'Orbigny, 1826–Jorissen (1987), p. 46, pl. 4, fig. 6.

Globobulimina affinis (d'Orbigny, 1839)–Parker (1958), p. 262, pl. 2, figs. 24–25.

Rectuvigerina phlegeri Le Calvez, 1959–Vénec-Peyré (1984), pl. 6, fig. 4.

Uvigerina bifurcata d'Orbigny, 1839–Van der Zwaan et al. (1986), p. 226, pl. 16, figs. 4–6; pl. 17, figs. 1–4.

Uvigerina mediterranea Hofker, 1932–Jorissen (1987), p. 46, pl. 1, fig. 2.

Uvigerina peregrina Cushman, 1923–Van Leeuwen (1989), p. 245, pl. 19, figs. 5–6.

Trifarina angulosa (Williamson, 1858)–Bremer et al. (1980), p. 18, pl. 2, fig. 4.

Suggrunda eckisi Natland, 1950–Burke et al. (1995), pl. 1, fig. 12.

Rutherfordoides rotundiformis (McCulloch, 1977)–Loeblich and Tappan (1987), p. 531, pl. 578, figs. 7–9.

Cancris auriculus (Fichtel and Moll, 1798)–Loeblich and Tappan (1987), p. 545, pl. 591, figs. 1–3.

Neoconorbina terquemi (Rzehak, 1888)–Jorissen (1987), p. 46, pl. 3, fig. 4.

Rosalina bradyi (Cushman, 1915)–Parker (1958), p. 268, pl. 3, figs. 37–38.

Hyalinea balthica (Schröeter, 1783)–Murray (1971), p. 173, pl. 72, figs. 5–8.

Planulina ariminensis d'Orbigny, 1826–Bremer et al. (1980), p. 23, pl. 3, figs. 5–7.

Cibicides lobatulus (Walker and Jacob, 1798)–Herb (1971), p. 296, pl. 2, fig. 11.

Cibicides pachydermus (Rzehak, 1886)–Jorissen (1987), p. 46, pl. 1, fig. 6.

Cibicides wuellerstorfi (Schwager, 1866)–Parker (1958), p. 275, pl. 4, figs. 41–42.

Planorbulina mediterranensis d'Orbigny, 1826–Parker (1958), p. 279, pl. 4, fig. 44.

Asterigerinata mamilla (Williamson, 1858)–Parker (1958), p. 264, pl. 3, figs. 5–6.

Nonion labradoricum (Dawson, 1860)–Hansen and Lykke-Andersen (1976), p. 23, pl. 21, figs. 5–8.

Nonionella turgida (Williamson, 1858)–Jorissen (1987), p. 46, pl. 4, figs. 11–13.

Astrononion stelligerum (d'Orbigny, 1839)–Loeblich and Tappan (1987), p. 619, pl. 694, figs. 1–2.

Melonis affinis (Reuss, 1851)–Wright (1978), p. 715, pl. 6, figs. 2–3.

Melonis barleeanum (Williamson, 1858)–Wright (1978), p. 715, pl. 6, fig. 4.

Chilostomella mediterranensis Cushman and Todd, 1949–Parker (1958), p. 273, pl. 4, fig. 24.

Gyroidina altiformis Stewart and Stewart, 1930–Jorissen (1987), p. 47, pl. 1, figs. 11–12.

Gyroidina orbicularis d'Orbigny, 1826–Jorissen (1987), p. 47, pl. 1, fig. 13.

Hanzawaia boueana (d'Orbigny, 1846)–Wright (1978), p. 715, pl. 5, figs. 12–14.

Appendix B. Supplementary data

Supplementary data associated with this article can be found, in the online version, at doi:10.1016/j.marmicro.2007.08.006.

References

Alavi, S.N., 1988. Late Holocene deep-sea benthic foraminifera from the Sea of Marmara. Marine Micropaleontology 13, 213–237.

Altenbach, A.V., Sarnthein, M., 1989. Productivity record in benthic foraminifera. In: Berger, W.H., Smetacek, V.S., Wefer, G. (Eds.), Productivity of the Ocean: Present and Past. Dahlem Conf. Wiley, New York, pp. 255–269.

Anastasakis, G.C., Stanley, D.J., 1984. Sapropels and organic-rich variants in the Mediterranean: sequence development and classification. In: Stow, D.A.V., Piper, D.J.W. (Eds.), Fine Grained Sediments: Deep-water Processes and Facies. Special Publications Geological Society, London, pp. 497–510.

Antoine, D., Morel, A., André, J.M., 1995. Algal pigment distribution and primary production in the eastern Mediterranean as derived from coastal zone scanner observations. Journal of Geophysical Research 100 (C8), 16.193–16.209.

Ayyad, S.N., Van der Zwaan, G.J., Hamama, H.H., 1991. The distribution of the Quaternary benthonic foraminifera in the eastern Mediterranean Sea. Mansoura Science Bulletin Special Issue 76–107 (Symposium of the Quaternary and Development in Egypt, 1991).

Barmawidjaja, D.M., Jorissen, F.J., Puscaric, S., Van der Zwaan, G.J., 1992. Microhabitat selection by benthic foraminifera in the northeast Adriatic Sea. Journal of Foraminiferal Research 22, 297–317.

Berger, W.H., Wefer, G., 1990. Export production: seasonality and intermittency, and paleoceanographic implications. Palaeogeography, Palaeoclimatology, Palaeoecology 89, 245–254 (Global Planetary Change Section).

Bernhard, J.M., 1992. Benthic foraminiferal distribution and biomass related to pore-water oxygen: central California continental slope and rise. Deep-Sea Research 39, 585–605.

Bernhard, J.M., 1996. Microaerophilic and facultative anaerobic benthic foraminifera: a review of experimental and ultrastructural evidence. Revue de Paléobiologie 15, 261–275.

Bernhard, J.M., Reimers, C.E., 1991. Benthic foraminiferal population fluctuations related to anoxia: Santa Barbara Basin. Biogeochemistry 15, 127–149.

Bizon, G., Bizon, J.J., 1984a. Distribution des foraminifères su plateau continental au large du Rhone. In: Bizon, Burollet (Eds.), Ecologie des microorganismes en Méditerranée occidentale « ECOMED ». Association française des Techniciens du Pétrole, Paris, pp. 84–94.

Bizon, G., Bizon, J.J., 1984b. Les foraminifères des sédiments profonds. In: Bizon, J.J., Burollet, P.F. (Eds.), Ecologie des microorganismes en Méditerranée occidentale (ECOMED). Association française des Techniciens du Pétrole, Paris, pp. 104–139.

Boltovskoy, E., Wright, R.H., 1976. Recent foraminifera. Junk, The Hague, 515 pp.

Bremer, M.L., Briskin, M., Berggren, W.A., 1980. Quantitative paleobathymetry and paleoecology of the late Pliocene–early Pleistocene foraminifera of Le Castella (Calabria, Italy). Journal of Foraminiferal Research 10 (l), 1–30.

Burke, S.K., Dunbar, R.B., Berger, W.H., 1995. Benthic and pelagic foraminifera of the Macoma Layer, Santa Barbara Basin. Journal of Foraminiferal Research 25 (2), 117–133.

Caralp, M.H., 1989. Abundance of *Bulimina exilis* and *Melonis barleeanum*: relationship to the quality of marine organic matter. Geo-Marine Letters 9, 37–43.

Casford, J.S.L., Rohling, E.J., Abu-Zied, R., Cooke, S., Fontanier, C., Leng, M., Lykousis, V., 2002. Circulation changes and nutrient concentrations in the Late Quaternary Aegean Sea: a non-steady state concept for sapropel formation. Paleoceanography 17, 14.1–14.11.

Casford, J.S.L., Rohling, E.J., Abu-Zied, R.H., Fontanier, C., Jorissen, F.J., Leng, M., Schmiedl, G., Thomson, J., 2003. A dynamic concept for eastern Mediterranean circulation and oxygenation during sapropel formation. Palaeogeography, Palaeoclimatology, Palaeoecology 190, 103–119.

Cita, M.B., 1973. Inventory of Biostratigraphical Findings and Problems. In: Ryan, W.B.F., Hsü, K.J., et al. (Eds.), Initial Reports of the DSDP, 13. U.S. Govt. Printing Office, Washington, D.C., pp. 1045–1074.

Cita, M.B., Zocchi, M., 1978. Distribution patterns of benthic foraminifera on the floor of the Mediterranean Sea. Oceanologica Acta 1 (4), 445–462.

Cita, M.B., Podenzani, M., 1980. Destructive effects of oxygen starvation and ash fall on benthic life: a pilot study. Quaternary Research 13, 230–241.

Corliss, B.H., 1985. Microhabitats of benthic foraminifera within deep-sea sediments. Nature 314, 435–438.

Corliss, B.H., 1991. Morphology and microhabitat preferences of benthic foraminifera from the northwest Atlantic Ocean. Marine Micropaleontology 17, 195–236.

Corliss, B.H., Chen, C., 1988. Morphotype patterns of Norwegian Sea deep-sea benthic foraminifera and ecological implications. Geology 16, 716–719.

Corliss, B.H., Emerson, S., 1990. Distribution of rose Bengal stained deep-sea benthic foraminifera from the Nova Scotian continental margin and Gulf of Maine. Deep-Sea Research 37, 381–400.

Cushman, J.A., 1932. The foraminifera of the Tropical Pacific collections of the "Albatross," 1899–1900. Pt. 1. Astrorhizidae to Trochamminidae, United States National Museum Bulletin, vol. 161, pp. 1–88.

De Rijk, S., Rohling, E.J., Hayes, A., 1999a. Onset of climatic deterioration in the eastern Mediterranean around 7 ky BP: micropalaeontological data from Mediterranean sapropel interruptions. Marine Geology 153, 337–343.

De Rijk, S., Troelstra, S.R., Rohling, E.J., 1999b. Benthic foraminiferal distribution in the Mediterranean Sea. Journal of Foraminiferal Research 29, 93–103.

De Rijk, S., Jorissen, F.J., Rohling, E.J., Troelstra, S.R., 2000. Organic flux control on bathymetric zonation of Mediterranean benthic foraminifera. Marine Micropaleontology 40, 151–166.

De Stigter, H.C., Jorissen, F.J., Van der Zwaan, G.J., 1998. Bathymetric distribution and microhabitat partitioning of live (rose Bengal stained) benthic foraminifera along a shelf to bathyal transect in the southern Adriatic Sea. Journal of Foraminiferal Research 28 (1), 40–65.

Edelman-Furstenberg, Y., Scherbacher, M., Hemleben, C., Almogi-Labin, A., 2001. Deep-sea benthic foraminifera from the central Red Sea. Journal of Foraminiferal Research 31 (1), 48–59.

Fontanier, C., Jorissen, F.J., Licari, L., Alexandre, A., Anschutz, P., Carbonel, P., 2002. Live benthic foraminiferal faunas from the Bay of Biscay: faunal density, composition and microhabitats. Deep-Sea Research I 49, 751–785.

Fontanier, C., Jorissen, F.J., Chaillou, G., David, C., Anschutz, P., Lafon, V., 2003. Seasonal and internannual variability of benthic foraminiferal faunas at 550 m depth in the Bay of Biscay. Deep-Sea Research I 50, 457–494.

Goldstein, S.T., Corliss, B.H., 1994. Deposit feeding selected deep-sea and shallow-water benthic foraminifera. Deep-Sea Research I 41, 229–241.

Gooday, A.J., 1986. Meiofaunal foraminiferans from the bathyal Porcupine Seabight (northeast Atlantic): size structure, standing stock, taxonomic composition, species diversity and vertical distribution in the sediment. Deep-Sea Research 33 (10), 1345–1373.

Gooday, A.J., 1988. A response by benthic foraminifera to the deposition of phytodetritus in the deep sea. Nature 332, 70–73.

Gooday, A.J., Turley, C.M., 1990. Responses by benthic organisms to inputs of organic material to the ocean floor: a review. Philosophical Transactions- Royal Society of London A331, 119–138.

Hansen, H.J., Lykke-Andersen, A.-L., 1976. Wall structure and classification of fossil and recent elphidiid and nonionid foraminifera. Fossils and Strata 10, 1–37.

Herb, R., 1971. Distribution of Recent Benthonic Foraminifera in the Drake Passage. In: Llana, G.A., Wallen, I.E (Eds.), Biology of the Antarctic Seas IV. Antarctic Research Series, 17, pp. 251–300.

Herguera, J.C., Berger, W.H., 1991. Paleoproductivity from benthic foraminifera abundance: glacial to interglacial change in the west-equatorial Pacific. Geology 19, 1173–1176.

Hughen, K.A., Baillie, M.G.L., Bard, E., Bayliss, A., Beck, J.W., Bertrand, C.J.H., Blackwell, P.G., Buck, C.E., Burr, G.S., Cutler, K.B., Damon, P.E., Edwards, R.L., Fairbanks, R.G., Friedrich, M., Guilderson, T.P., Kromer, B., McCormac, F.G., Manning, S.W., Bronk Ramsey, C., Reimer, P.J., Reimer, R.W., Remmele, S., Southon, J.R., Stuiver, M., Talamo, S., Taylor, F.W., van der Plicht, J., Weyhenmeyer, C.E., 2004. Marine04, Marine radiocarbon age calibration, 26–0 ka BP. Radiocarbon 46, 1059–1086.

Jannink, N.T., Zachariasse, W.J., Van der Zwaan, G.J., 1998. Living (Rose Bengal stained) benthic foraminifera from the Pakistan continental margin (northern Arabian Sea). Deep-Sea Research I 45, 1483–1513.

Jones, R.W., 1994. The "Challenger Foraminifera". Oxford University Press for the Natural History Museum, 149 pp.

Jorissen, F.J., 1987. The distribution of benthonic foraminifera in the Adriatic Sea. Marine Micropaleontology 12, 21–48.

Jorissen, F.J., 1988. Benthic foraminifera from the Adriatic Sea; principles of phenotypic variations. Utrecht Micropaleontological Bulletins 37 (176 pp.).

Jorissen, F.J., 1999a. Benthic foraminiferal successions across Late Quaternary Mediterranean Sapropels. Marine Geology 153, 91–103.

Jorissen, F.J., 1999b. Benthic foraminiferal microhabitats below the sediment–water interface. In: Sen Gupta, B.K. (Ed.), Modern Foraminifera. Kluwer Academic publishers, Dordrecht, pp. 161–179.

Jorissen, F.J., Wittling, I., 1999. Ecological evidence from taphonomical studies; living-dead comparisons of benthic foraminiferal faunas off Cape Blanc (NW Africa). Palaeogeography, Palaeoclimatology, Palaeoecology 149, 151–170.

Jorissen, F.J., De Stigter, H.C., Widmark, J.G.V., 1995. A conceptual model explaining benthic foraminifera microhabitats. Marine Micropaleontology 26, 3–15.

Jorissen, F.J., Fontanier, C., Thomas, E., 2007. Paleoceanographical proxies based on deep-sea benthic foraminiferal assemblage characteristics. In: Hillaire-Marcel, C., De Vernal, A. (Eds.), Proxies in Late Cenozoic Paleoceanography. Elsevier Publishers, pp. 277–340.

Katz, M.E., Thunell, R.C., 1984. Benthic foraminiferal biofacies associated with middle Miocene to early Pliocene oxygen-deficient conditions in the eastern Mediterranean. Journal of Foraminiferal Research 14 (3), 187–202.

Keller, J., Ryan, W.B.F., Ninkovich, D., Altherr, R., 1978. Explorative volcanic activity in the Mediterranean over the past 200,000 yr as recorded in deep-sea sediments. Geological Society of America Bulletin 89, 591–604.

Kidd, R.B., Cita, M.B., Ryan, W.B.F., 1978. Stratigraphy of the Eastern Mediterranean Sapropel Sequences Recovered during DSDP LEG 42A and Their Paleoenvironmental Significance. In: Hsü, K.J., Montadert, L., et al. (Eds.), Initial Reports of the DSDP, 42. U.S. Govt. Printing Office, Washington, D.C., pp. 421–443.

Lander Rasmussen, T., 1991. Benthonic and planktonic foraminifera in relation to the Early Holocene stagnations in the Ionian basin, central Mediterranean. Boreas 20, 357–376.

Lankford, R.R., Phleger, F.B., 1973. Foraminifera from the nearshore turbulent zone, western North America. Journal of Foraminiferal Research 3 (3), 101–132.

Loeblich, A.R., Tappan, H., 1987. Foraminiferal Genera and Their Classification, 2 v. vanNostrand Reinhold, New York. (970 pp.).

Lohmann, G.P., 1978. Abyssal benthonic foraminifera as hydrographic indicators in the western South Atlantic Ocean. Journal of Foraminiferal Research 8 (1), 6–34.

Loubere, P., 1991. Deep-sea benthic foraminiferal assemblage response to a surface ocean productivity gradient: a test. Paleoceanography 6, 193–204.

Lutze, G.F., Coulbourn, W.T., 1984. Recent benthic foraminifera from the continental margin of northwest Africa: community structure and distribution. Marine Micropaleontology 8, 361–401.

Mackensen, A., Douglas, R., 1989. Down-core distribution of live and dead deep-water benthic foraminifera in box cores from the Weddell Sea and California borderland. Deep-Sea Research 36, 879–900.

Mackensen, A., Schumacher, S., Radke, J., Schmidt, D.N., 2000. Microhabitat preferences and stable carbon isotopes of endobenthic foraminifera: clue to quantitative reconstruction of oceanic new production? Marine Micropaleontology 40, 233–258.

Mangini, A., Schlosser, P., 1986. The formation of eastern Mediterranean sapropels. Marine Geology 72, 115–124.

McCoy, F.W., 1980. The upper Thera (Minoan) ash in deep-sea sediments: distribution and comparison with other ash layers. In: Dumas, C. (Ed.), Thera and Aegean World. Proceedings 2° International Scientific Congress on the Volcano of Thera, Greece 2, 57–78.

Mercone, D., Thomson, J., Croudace, I.W., Siani, G., Paterne, M., Troelstra, S., 2000. Duration of S1, the most recent sapropel in the eastern Mediterranean Sea, as indicated by accelerator mass spectrometry radiocarbon and geochemical evidence. Paleoceanography 15 (3), 336–347.

Mercone, D., Thomson, J., Abu-Zied, R.H., Croudace, I.W., Rohling, E.J., 2001. High-resolution geochemical and micropalaeontological profiling of the most recent eastern Mediterranean sapropel. Marine Geology 177, 25–44.

Miller, K.G., Lohmann, G.P., 1982. Environmental distribution of recent benthic foraminifera on the northeast United States

continental slope. Geological Society of America Bulletin 93, 200–206.
Morigi, C., Jorissen, F.J., Gervais, S., Guichard, S., Borsetti, A.M., 2001. Benthic foraminiferal faunas in surface sediments off NW Africa: relationship with organic matter flux tot he ocean floor. Journal of Foraminiferal Research 31, 350–368.
Mullineaux, L.S., Lohmann, G.P., 1981. Late Quaternary stagnations and recirculation of the eastern Mediterranean, changes in the deep water recorded by fossil benthonic foraminifera. Journal of Foraminiferal Research 11 (1), 20–39.
Murray, J.W., 1971. An Atlas of British Recent foraminiferids. Heineman Educational Books, London. (1–95 pls, 244 pp.).
Myers, P.G., Haines, K., Rohling, E.J., 1998. Modeling the paleocirculation of the Mediterranean: the last glacial maximum and the Holocene with emphasis on the formation of sapropel S1. Paleoceanography 13 (6), 586–606.
Narcisi, B., Vezzoli, L., 1999. Quaternary stratigraphy of distal tephra layers in the Mediterranean—an overview. Global and Planetary Change 21, 31–50.
Nijenhuis, I.A., Schenau, S.J., Van der Weijden, C.H., Hilgen, F.J., Lourens, L.J., Zachariasse, W.J., 1996. On the origin of upper Miocene sapropelites: a case study from the Faneromeni section, Crete (Greece). Paleoceanography 11 (5), 633–645.
Nolet, G.J., Corliss, B.H., 1990. Benthic foraminiferal evidence for reduced deep-water circulation during sapropel deposition in the eastern Mediterranean. Marine Geology 94, 109–130.
Parker, F.L., 1958. Eastern Mediterranean foraminifera, sediment cores from the Mediterranean Sea, and the Red Sea. Reports of the Swedish Deep-Sea Expedition, 1947-1948 8 (4), 219–285.
Phleger, F.B., Parker, F.L., Pierson, J.F., 1953. North Atlantic foraminifera. Reports of the Swedish Deep-Sea Expedition, 1947-1948 7 (1), 1–122.
Pichler, H., Friedrich, W., 1976. Radiocarbon dates of Santorini volcanics. Nature 262, 373–374.
Rohling, E.J., 1994. Review and new aspects concerning the formation of eastern Mediterranean sapropels. Marine Geology 122, 1–28.
Rohling, E.J., Gieskes, W.W.C., 1989. Late Quaternary changes in Mediterranean Intermediate Water density and formation rate. Paleoceanography 4, 531–545.
Rohling, E.J., De Stigter, H.C., Vergnaud-Grazzini, C., Zaalberg, R., 1993. Temporary repopulation by low oxygen tolerant benthic foraminifera within an Upper Pliocene sapropel: evidence for the role of oxygen depletion in the formation of sapropels. Marine Micropaleontology 22, 207–219.
Rohling, E.J., Jorissen, F.J., De Stigter, H.C., 1997. 200 Year interruption of Holocene sapropel formation in the Adriatic Sea. Journal of Micropaleontology 16, 97–108.
Rohling, E.J., Mayewski, P.A., Abu-Zied, R.H., Casford, J.S.L., Hayes, A., 2002. Holocene atmosphere–ocean interactions: records from Greenland and the Aegean Sea. Climate Dynamics 18, 587–593.
Ross, C.R., Kennett, J.P., 1984. Late Quaternary paleoceanography as recorded by benthonic foraminifera in Strait of Sicily sediment sequences. Marine Micropaleontology 8, 315–336.
Rossignol-Strick, M., 1985. Mediterranean Quaternary sapropels, an immediate response of the African monsoon to variation of insolation. Palaeogeography, Palaeoclimatology, Palaeoecology 49, 237–263.
Sen Gupta, B.K., Machain-Castillo, M.L., 1993. Benthic foraminifera in oxygen-poor habitats. In: Langer, M.R. (Ed.), Foraminiferal Microhabitats. Marine Micropaleontology, 20, pp. 183–201.
Sigl, W., Chamley, H., Fabricius, F., D'Argoud, G.G., Müller, J., 1978. Sedimentology and Environmental Conditions of Sapropels. In: Hsü, K.J., Montadert, L., et al. (Eds.), Initial Reports of the DSDP, 42. U.S. Govt. Printing Office, Washington, D.C., pp. 445–465.
Stuiver, M., Reimer, P.J., Reimer, R.W., 2005. CALIB 5.0. [WWW program and documentation].
Thiel, H., 1983. Meiobenthos and Nanobenthos of the Deep Sea. In: Rowe, G.T. (Ed.), Deep-sea Biology. The Sea, 8, pp. 167–230.
Van der Zwaan, G.J., 1980. The impact of climatic changes on deep sea benthos: a micropaleontological investigation of a deep sea core from the SE Adriatic. Proceedings of the Koninklijke Nederlandse Akademie van Wetenschappen. Series B 83 (4), 379–397.
Van der Zwaan, G.J., Jorissen, F.J., 1991. Biofacial patterns in river-induced shelf anoxia. In: Tyson, R.V., Pearson, T.H. (Eds.), Modern and Ancient Continental Shelf Anoxia. Geological Society of London Special Publication, 58, pp. 65–82.
Van der Zwaan, G.J., Jorissen, F.J., Verhallen, P.J.J.M., Von Daniels, C.H., 1986. Atlantic–European Oligocene to Recent *Uvigerina*. Utrecht Micropaleontological Bulletins 35 (240 pp.).
Van Leeuwen, R.J.W., 1989. Sea-floor distribution and Late Quaternary faunal patterns of planktonic and benthic foraminifera in the Angola Basin. Utrecht Micropaleontological Bulletins 38 287 pp.
Van Straaten, L.M.J.U., 1972. Holocene stages of oxygen depletion in deep waters of the Adriatic Sea. In: Stanley, D.J. (Ed.), The Mediterranean Sea. Dowden, Hutchinson and Ross, Stroudsburg, Pa., pp. 631–643.
Vénec-Peyré, M.-T., 1984. Étude de la distribution des foraminifères vivant dans la baie de Banyuls-sur-Mer. In: Bizon, J.J., Burollet, P.F. (Eds.), Ecologie des microorganismes en Méditerranée occidentale (ECOMED). Association française des Techniciens du Pétrole, Paris, pp. 60–80.
Vismara-Schilling, A., Coulbourn, W.T., 1991. Benthic foraminiferal thanatofacies associated with late Pleistocene to Holocene anoxic events in the eastern Mediterranean Sea. Journal of Foraminiferal Research 21 (2), 103–125.
Wright, R., 1978. Neogene Benthic Foraminifers from DSDP Leg 42A, Mediterranean Sea. In: Hsü, K.J., Montadert, L., et al. (Eds.), Initial Reports of the DSDP, 42. U.S. Govt. Printing Office, Washington, D.C., pp. 709–726.